SAPHYRE

Contract No. FP7-ICT-248001

Test Case Implementation and Evaluation on the Demonstrator Testbed (initial)
D6.3a

Contractual date:	M24
Actual date:	M25
Authors:	Jian Luo, Andreas Kortke, Volker Jungnickel, Finn-Arne Böhner, Rami Mochaourab, Eduard Jorswieck, Johannes Lindblom, Eleftherios Karipidis, Erik G. Larsson, Jianhui Li, Jianshu Zhang, Martin Haardt, Pavel Procházka, Jan Sýkora
Participants:	FhG, TUD, LiU, TUIL, CTU
Work package:	WP6
Security:	Public
Nature:	Report
Version:	1.1
Number of pages:	93

Abstract

This document describes the initial test case implementation and evaluation on the demonstrator platforms within WP6.

Keywords

Scenario, test case, evaluation, demonstrator platform, proof-of-concept, algorithm verification.

Executive Summary

The SAPHYRE (Sharing Physical Resources – Mechanisms and Implementations for Wireless Networks) project investigates voluntary physical resource sharing in wireless networks. Within this project, effective resource sharing mechanisms will be developed, which should help to enhance spectral efficiency, coverage, user satisfaction and operator revenue. Two of the most important contributions of SAPHYRE are advanced signal processing and coding algorithms (WP3) as well as cross-layer optimization algorithms (WP4), which are enabling techniques for resource sharing. However, algorithms that are designed under idealized assumptions may not work in real wireless systems, probably due to the influence of non-ideal system conditions. In order to solve this problem, a demonstrator platform has been developed, which allows flexible and efficient Hardware-in-the-Loop (HIL) tests. HIL tests are signal transmission tests which involve real RF hardware and most of the practical system conditions and thus can provide proof-of-concept. For this purpose, a HIL demonstrator platform was set up which allows HIL test of algorithms. During the first two years, four representative scenarios have been selected for implementation and evaluation on the demonstrator platform. The corresponding description, implementation details and the initial results are reported in this deliverable. This deliverable first gives an overview of the selected scenarios and test cases for implementation. Afterwards, the scenario implementation work flow is described, which includes the interaction between WP6 and the other WPs. The important functionalities of the demonstrator platform are also listed. Afterwards, the test case implementation and evaluation of the four scenarios are reported. The first one is the spectrum sharing scenario without base-station collocation. The second one is the full sharing (spectrum and base-station) scenario. In both these scenarios, advanced beam-forming techniques were applied to enable SAPHYRE gains with sharing. HIL test results show that by sharing the spectrum, considerable gain in rate/throughput can be achieved. Moreover, especially in the first scenario, a number of advanced beam-forming algorithms have been applied. The third and the fourth scenarios are both relay sharing scenarios, while the third scenario consists of a “butterfly” network, the fourth scenario consists a two-way-relaying network. In the third case, advanced network coding techniques were applied to enable spectrum sharing. In the fourth case, advanced multi-antenna techniques were applied at the relay to allow spectrum sharing gain. HIL test results has verified the sharing gain in the third scenario. For the fourth, the HIL test remains future work. Further improvements of the implemented scenarios and extended HIL tests are expected in the future.

In order to significantly improve the visibility of the SAPHYRE project towards the industry, a subset of the selected scenarios will be implemented on a further demonstrator platform, i.e. the Berlin LTE-Advanced testbed provided by FhG. The spectrum sharing scenario has already been selected as an initial scenario. An initial test case has been defined and partly implemented.

Contents

Abbreviations

AF	Amplify and Forward
ACC	Automatic Gain Control
ANOMAX	Algebraic NOrm-MAXimizing transmit strategy
AWGN	Additive White Gaussian Noise
BB	Baseband
BC	BroadCast
BD	Block Diagonalization
BER	Bit Error Rate
BF	BeamForming
BS	BaseStation
CF	Compress and Forward
CFO	Carrier Frequency Offset
CoBF	Cooperative Beam-Forming
CoBG	Cooperative BarGaining
CP	Cyclic Prefix
CPE	Common Phase Error
CQI	Channel Quality Indicator
CSI	Complimentary Side Information
CSI	Channel State Information
DAC	Digital-to-Analog Converter
DF	Decode and Forward
DFT	Discrete Fourier Transform
EMBF	Eigen-Mode BeamForming
HDF	Hierarchical Decode and Forward
HIL	Hardware-In-the-Loop
IOI	Inter-Operator Interference
LPF	Low-Pass Filter
LTE	Long Time Evolution
MAC	Medium Access Control layer
MAC-phase	Multiple ACcess phase
MIMO	Multiple Input Multiple Output
ML	Maximum Likelihood
MMSE	Minimum Mean Square Error
MRT	Maximum Ratio Transmission
NE	Nash Equilibrium
OFDM	Orthogonal Frequency-Division Multiplexing
OPR	Operator

PHY	Physical layer
RBD	Regularized Block Diagonalization
RF	Radio Frequency
Rx	Receiver
SC	SubCarrier
SIC	Successive Interference Cancellation
SINR	Signal-to-Interference-and-Noise Ratio
SNR	Signal-to-Noise Ratio
SP	Signal Processing
SVD	Singular-Value-Decomposition
TSE	Time Synchronization Error
TNR	Tx power to Noise power Ratio
TWR	Two Way Relay
Tx	Transmitter
UT	User-Terminal
WP	Work Package
ZF	Zero Forcing

1 Introduction

The SAPHYRE (Sharing Physical Resources – Mechanisms and Implementations for Wireless Networks) project investigates voluntary physical resource sharing in wireless networks. Within this project, effective resource sharing mechanisms will be developed, which should help to enhance spectral efficiency, coverage, user satisfaction and operator revenue. Two of the most important contributions of SAPHYRE are advanced signal processing and coding algorithms (WP3) as well as cross-layer optimization algorithms (WP4), which are enabling techniques for resource sharing. These techniques have been reported in [10, 9, 15, 27, 5, 31, 14, 21, 22, 23] as well as the deliverables D3.1a [4], D3.2a [32], D4.1 [1] etc.

However, as stated in [30, 34] etc., algorithms that are designed under idealized assumptions may not work in real wireless systems, probably due to the influence of non-ideal system conditions e.g. RF impairments [2] and real wave propagation environment. In order to solve this problem, a demonstrator platform has been developed, which allows flexible and efficient Hardware-in-The-Loop (HIL) tests. HIL tests are signal transmission tests which involve real RF hardware and most of the practical system conditions. With HIL tests, practical problems and constraints can be identified in the design stage of resource sharing algorithms, so that they can be optimized. Furthermore, an algorithm that performs well in HIL test can be declared as feasible. In other words, HIL test provides proof-of-concept. The description of this demonstrator platform can be found in the deliverable D6.2 [16], which includes the structure of the platform, the working principle, the configuration modes, the functionalities and the operation parameters.

The HIL test and verification of the SAPHYRE algorithms are carried out in the following steps: 1)Selection of representative scenarios and test cases; 2)Mapping and implementation of the scenarios, test cases and the corresponding algorithms on the demonstrator platform; 3) HIL transmission experiments; 4) Evaluation of the experiment results.

In order to further improve the visibility of the SAPHYRE project towards the industry, a subset of the selected scenarios will be implemented on a further demonstrator platform i.e. the Berlin LTE-Advanced testbed provided by FhG.

During the first two years of the SAPHYRE project, four initial scenarios as well as the corresponding test cases have been selected. Some enabling algorithms for resource sharing have also been developed for these scenarios. These scenarios include: 1)Spectrum sharing scenario; 2) Full sharing (spectrum and infrastructure sharing) scenario; 3)Relay (and spectrum) sharing scenario in “butterfly” network; 4)Relay

(and spectrum) sharing scenario in Two-Way-Relaying (TWR) network. The initial implementation as well as the HIL test of these scenarios have been carried out. The initial HIL results are available and will be shown in this deliverable. Furthermore, the spectrum sharing scenario will be implemented on the LTE-Advanced testbed. The initial experimental setup and implementation will also be reported.

This deliverable is organized as follows: Chapter 2 describes the overview of the selected scenarios and test cases for implementation and evaluation on the demonstrator platform. Chapter 3 describes the scenario and test case implementation work flow. Chapter 4 and Chapter 5 describe the important functionalities of the HIL-demonstrator and the LTE-Advanced testbed. Chapter 6 describes the initial implementation, evaluation and test results of the scenarios on the HIL-demonstrator platform, including the spectrum sharing scenario (SC2-TA, Sec. 6.1), the full sharing (spectrum- and infrastructure sharing, SC1-TB, 6.2), the relay sharing scenario in "butterfly" network (SC1-TC-I, Sec. 6.3) and the relay sharing scenario in Two-Way-Relaying (TWR) network (SC1-TC-II,Sec. 6.4). Chapter 7 describes the initial implementation on the LTE-Advanced testbed. Chapter 8 concludes this deliverable. A part of the results in this deliverable is also reported in the papers [19, 18].

2 Overview of Selected Scenarios and Test Cases for Implementation

For the implementation and evaluation on the demonstrator platform, four scenarios have been selected out of those defined in D3.3a [3] and D5.1a [6]. All these scenarios have been mentioned in the deliverable D6.1a [20]. However, we have extended the circumference of these scenarios and will give a more compact and complete view about these scenarios in this chapter. Note that these four scenarios are representative throughout the whole SAPHYRE project and are observed in most of the work packages. Furthermore, they are most challenging in terms of signal processing and coding as well as cross-layer design. These scenarios are listed below:

2.1 Scenario SC2-TA: Spectrum Sharing

In this scenario, several operators share the spectrum. The BSs of the different operators are not shared. The BSs of all operators transmit signal at the same time within the same spectrum for their dedicated UTs. In SAPHYRE, we have defined two classes of spectrum sharing: orthogonal spectrum sharing and non-orthogonal spectrum sharing. With orthogonal spectrum sharing, orthogonal frequency resources are allocated to different operators from a common spectrum pool. In this case, no interference is generated between the operators. Advanced resource allocation techniques can be used to enhance system throughput. With non-orthogonal spectrum sharing, each frequency resource can be simultaneously used by multiple operators. In this case, inter-operator interference exists, which should be managed using advanced signal processing techniques (e.g. advanced Beam-Forming, BF, techniques). With adequate techniques, the system throughput as well as the spectral efficiency can be maximized. For this scenario, the test cases include the comparison between non-sharing and sharing cases as well as between different advanced signal processing techniques for spectrum sharing. More detailed description can be found in Sec. 6.1.

2.2 Scenario SC1-TB: Full Sharing

In this scenario, several operators share both the spectrum and the BSs i.e. the signals of different operators are transmitted via the same antennas at a BS. The two classes of spectrum sharing also apply for this scenario: orthogonal spectrum shar-

ing and non-orthogonal spectrum sharing. With orthogonal spectrum sharing, the signals of different operators are multiplexed in the spectrum. With non-orthogonal spectrum sharing, the signals of multiple operators are transmitted with the same spectrum resource via the same antennas. In this case, advanced signal processing techniques (e.g. advanced precoding techniques) can be used to allow the simultaneous transmission and maximize the system throughput. For this scenario, the test cases include the comparison between non-sharing and sharing cases as well as between different advanced signal processing techniques for full sharing. More detailed description can be found in Sec. 6.2.1.

2.3 Scenario SC1-TC-I: Relay Sharing in "Butterfly" Network

In this scenario, several operators share both the spectrum and a relay station. This scenario consists of a "butterfly" network topology, where several independent data sources of different operators should transmit data to the same number of destinations, respectively, via two-phase relaying transmission. The data sources as well as the data destinations can be either BSs or UTs. The two phases of the relaying transmission are the Multiple Access (MAC) phase and the the BroadCast (BC) phase. In the MAC phase, the data sources transmit data to the relay and to the destinations, respectively. In this scenario, we assume that there is no direct link between a source and its dedicated destination. In the BC phase, the relay transmits data to both destinations. The destinations try to decode the dedicated data. Since both relay and spectrum are shared, the data streams of different sources will be superimposed at the relay and cause interference to each other. To manage such interference and achieve maximum capacity, sophisticated relaying strategy and network coding techniques can be applied. For this scenario, the test cases include the comparison between cases with and without spectrum sharing as well as between different relaying/network coding strategies for spectrum and relay sharing. More detailed description can be found in Sec. 6.3.

2.4 Scenario SC1-TC-II: Relay Sharing in Two-Way-Relaying Network

In this scenario, several operators also share both the spectrum and a relay station. However, unlike the scenario SC1-TC-I, a Two-Way-Relaying (TWR) network is observed. In this scenario, multiple communication partners (UT pairs) owned by different operators use one relay station (possibly owned by another operator/virtual operator) to bidirectionally exchange information using the same spectrum. All UTs as well as the relay station have multiple antennas and operate in half-duplex mode. The TWR also consists of two transmission phase: the MAC-phase and the BC-

phase. In the MAC-phase, all UTs transmit data to the relay. In the BC-phase, the relay broadcast data to all UTs. This broadcast data was calculated by the relay according to its received data in the MAC-phase. Since both the relay and the spectrum are shared, inter-operator interference exists. Thus, advanced signal processing techniques should be applied at the relay to manage the interference they cause to each other according to their voluntary agreements. For this scenario, the test cases include the comparison between cases with and without spectrum sharing as well as between different relaying/network coding strategies for spectrum and relay sharing. More detailed description can be found in Sec. 6.4.

3 Scenario Implementation Work Flow

After the scenarios are selected, they are implemented and evaluated on the demonstrator platform via eight steps, which are described as follows:

1. **Raw implementation of algorithms:** The project partners of WP3 and WP4 provide initial implementation of the enabling algorithm in different scenarios. Such implementations are carried out under ideal assumptions e.g. single carrier transmission, flat-fading channels, perfect time synchronization etc. They will be used as a reference for the implementation on the demonstrator platform.
2. **Scenario mapping and initial implementation on the demonstrator platform:** The selected scenarios are mapped to the demonstrator platform. The raw implementation of the algorithms in these scenarios are used as a reference for the implementation on the demonstrator platform, which considers the practical implementation constraints e.g. multi-carrier transmission, frequency selectivity of the channels, scaling of signal amplitudes for the DAC, time synchronization error etc.;
3. **Pre-simulation with the implemented algorithms:** With the developed demonstrator platform, signal transmission can be carried out both in software and in hardware. In the early implementation stage, pre-simulation of the implemented algorithms are carried out with software transmissions. Note that even with software transmission, a number of practical constraints are already included e.g. frequency selective channels, DAC clipping, time synchronization error etc. Usually, problems of the algorithms under such constraints will appear. Such problems are fed back to the project partners of WP3 or WP4 for further improvement and optimization of the algorithms. The improvement and optimization can be done via cooperation of WP3/WP4 with WP6.
4. **Iterative improvement of the algorithms:** After the raw algorithms are improved by the WP3/WP4 partners, they are used as references to improve the implementation on the demonstrator platform. Then, the pre-simulation is performed again to check for further practical problems. The last two steps are repeated until all the practical problems are solved.
5. **HIL transmission experiment of the algorithms:** In this step, the implemented scenarios are run on real hardware. HIL transmission experiments are carried out to further test the implemented algorithms. The HIL transmission results are fed back to the project partners of WP3/WP4 for further

evaluation. Usually, additional hardware related problems can appear, which needs improvement of the algorithm or the implementation.

6. **Iterative improvement of the algorithm implementation:** The project partners of WP3/WP4 provide feedback according to the evaluation of the HIL experiment results. According to these feedbacks and analysis of the implementation, either the algorithm itself or the implementation manner may be improved. This experiment-and-feedback process is continued until satisfactory results are obtained by the HIL transmission experiment.

Fig. 3.1 illustrates the work flow described above.

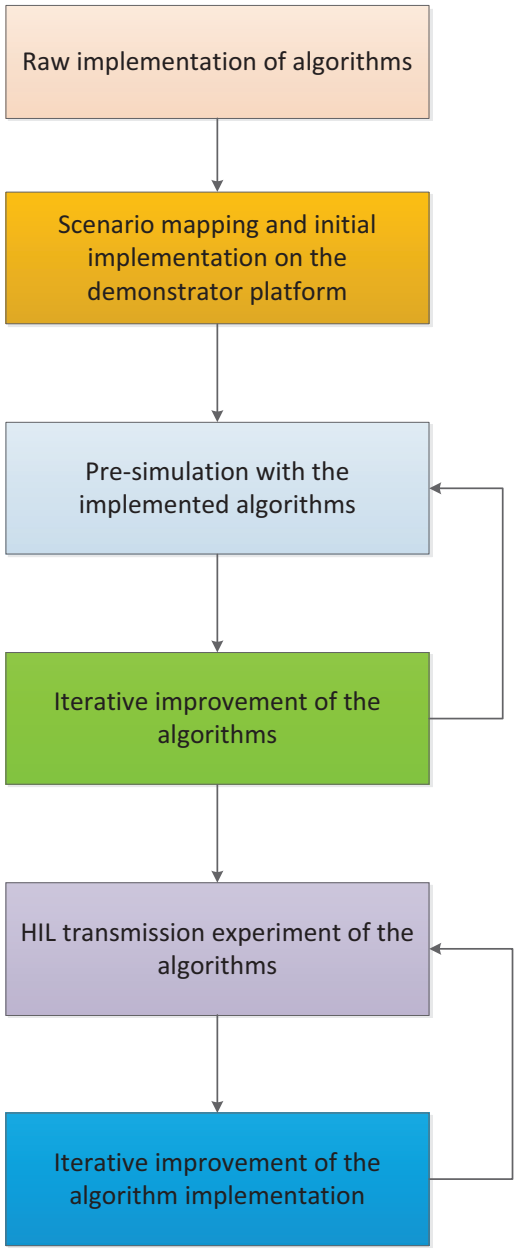

Figure 3.1: Workflow of scenario implementation.

4 Functionalities of the HIL-Demonstrator Platform

4.1 The Flexible and Reconfigurable HIL-Test Framework

A flexible and reconfigurable HIL-test framework has been developed for testing resource sharing mechanisms on the demonstrator platform. Fig. 4.1 shows the block diagram of this framework, which consists mainly of the transmitter part, the channel part, the receiver part and a number small parts realizing other functionalities like Automatic Gain Control (AGC), channel emulator control, multi-stage transmission mapping etc. In the practice, this frame work has to be adapted (modification, restructuring and extension) for each scenario. This frame work allows the following advantages:

- Efficient integration of new algorithms in a certain scenario. As long as the framework is already adapted for a scenario and the first algorithm has been integrated, new algorithms requiring the same interfaces can be efficiently integrated. But if new interface is required by a new algorithm (e.g. the game theoretical BF algorithms in scenario SC2-TA require rate estimation values, which were not required by the BD algorithm. This requires implementation of new interfaces). Accordingly in Fig. 4.1, mainly the blocks "advanced precoding algorithm" and "advanced decoding/relaying algorithm" have to be extended.
- This HIL-test framework allows efficient switching between different channel propagation environments, including the MATLAB software channel, the RF cable network (with precoded MATLAB channels in the transmitted signals), the channel emulator and the 60 GHz free space propagation channel. At the early algorithm implementation stage, pre-simulations can be carried out using the MATLAB software channels to identify preliminary implementation problems. Note that the use of MATLAB software channels is independent of the demonstrator hardware platform and thus, can be easily deployed by the individual project partners for preliminary tests of algorithms. The switching between different RF transmission channels allows to investigate the algorithms in different aspects. With RF cable network and the channel emulator, reproducible results can be produced and performance curves can be obtained to support theoretical and systematical algorithm test. With the 60 GHz free space propagation channel, the algorithms can be verified under the most realistic conditions.

- Easy adjustment of various parameters including mapping parameters (on the platform), platform parameters (e.g. carrier frequency, bandwidth), scenario parameters, signal parameters and evaluation parameters. By defining virtual- and physical Tx-Rx pairs, the mapping of the scenario to the demonstrator platform can be very efficient. Moreover, the scenario parameters can be flexibly configured e.g. the number of Tx/Rx antennas (but depending on the RF signal transmission mode and the number of available physical transmitters and receivers). The evaluation is also very flexible. In each transmission loop, some intermediate measurement results can be shown in live, e.g. the spectrum of the transmitted signals, the received signal samples, the estimated channel frequency response, the received signal constellation etc.

4.2 Important Functionalities of the Demonstrator Platform

For the implementation of the selected scenarios and systematical tests of resource sharing algorithms, the following functionalities of the demonstrator are very important:

- **Different RF signal transmission modes:** As mentioned in Sec. 4.1 and described in the deliverable D6.2 [16], three RF signal transmission modes are provided by the demonstrator platform: the RF cable network mode, the channel emulator mode and the 60 GHz free space transmission mode. While the first two modes provide reproducible results and are suitable for analysis and evaluation of resource sharing mechanisms, the 60 GHz transmission mode is suitable for live demonstration, where real radio channel effects can be shown.
- **Multi-stage transmission mapping:** As described in Sec. 3.2 of the deliverable D6.2 [16], multi-stage transmission mapping can be used in combination with the first two RF signal transmission modes. With this multi-stage transmission mapping, networks with larger Tx/Rx numbers than the number of available physical Tx/Rx can be simulated with HIL.
- **Multi-path channel effect:** In the RF cable network transmission mode, multi-path channels are generated by pre-distorting the transmitted signals in MATLAB. The impulse response of these channels are convolved with the corresponding Tx signals before they are transmitted. In the channel emulator mode, multi-path channel realizations are generated within the channel emulator. The channel effect on the modulated RF signal is accomplished in the channel emulator. In the 60 GHz transmission mode, the channels are real multi-path radio channels, which depends on the wave propagation environment.

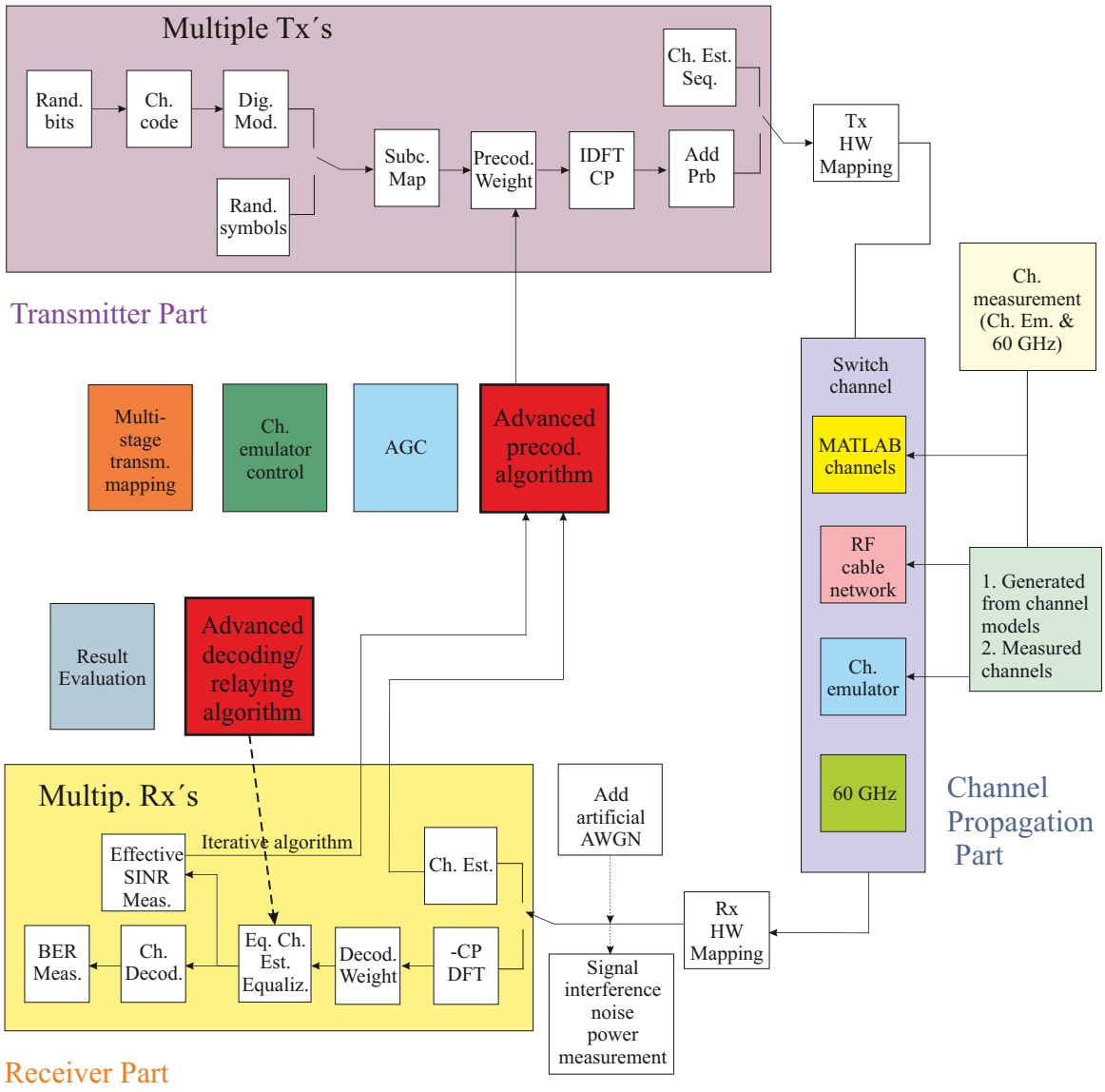

Figure 4.1: Block-diagram of the HIL-test framework

- **Remote Control and Different Operational Modes of the Channel Emulator:** The channel emulator is integrated to the demonstrator platform via remote control. The remote control is mainly done via the Ethernet connection between the central controller PC and the channel emulator. The remote control includes connection establishment, channel emulation setup (channel emulation file, input- and output gains/attenuations etc.), channel realization control and connection closure. For the channel realization control, two operation modes are implemented:

  1. **Stepping Mode:** Increments of the channel realization number is controlled by the Ethernet interface via the "STEP" or "GO TO" functions (see reference manual of the Elektrobit F8 channel emulator[1]). First, the central controller software sends a command to inform the channel emulator to increase the channel realization number (go to the next channel realization) or to go to a certain channel realization. Afterwards, the channel realization remains constant, as the global signal transmission is triggered. In this way, block-fading channels can be realized, which is very favorable for algorithm test.
  2. **Trigger-and-Run Mode:** In this case, the updating of the channel realizations is not controlled by the Ethernet connection but by an additional external trigger signal. After connection establishment, the channel realization stays constant until the external trigger signal is active. During the active duration of the external trigger signal, the channel realizations are updated according to the predefined fading- and mobility parameters. As soon as the external signal returns to inactive state, the channel realization becomes constant again. In this way, fast fading channels can be realized, which can be used for further test of the algorithms.

- **Channel estimation:** Usually, perfect channel knowledge can be assumed in the theoretical derivation of resource sharing algorithms. However, this is not realistic. In practice, the signal propagation channel also includes influence of all relevant hardware components (BB analog components and RF components). Thus, even if the equivalent BB impulse response of the radio channel is known (which is the case of the first of the second RF signal transmission modes), the total channel characteristics are generally unknown. Thus, channel estimation has to be carried out. In our HIL test, we apply the Maximum-Likelihood (ML) channel estimation of [17] to obtain the channel coefficients. This scheme is designed for MIMO transmissions and can be easily extended to the selected scenarios. The quality of the channel estimates can be adjusted by changing the pilot sequence length.

- **SNR adjustment:** The receive SNR can be adjusted by two methods. The first method is to variate the gain factors of the variable gain amplifiers at the modulators as well as those of the LNA at the receivers. The second method

[1] Elektrobit System Test Ltd., Finland, www.elektrobit.com.

is to add Additive White Gaussian Noise (AWGN) to the received signals in MATLAB. Generally, the first method may include more practical effects e.g. colored noise than the second method. However, the second method also provides a good proof-of-concept under influence of most of the hardware effects. Both methods can be combined to adjust the receive SNR.

- **Signal power, interference power and the noise power measurement:** Generally, for performance evaluation of the resource sharing algorithms, the value of the received SNR is required, which is generally not exactly known. Thus, additional pilot sequences are transmitted to estimate the SNR value as well as the SINR value. For scenarios with interference links, signal power and interference power should be distinguished. For this purpose, different BSs should transmit the pilot sequence alternately i.e. when one BS transmits, the other BSs should not transmit.
- **Signal bandwidth adjustment:** The adjustable range of the sampling clock of the demonstrator platform is between 300 MHz and 500 MHz, resulting in the maximum signal bandwidth between 150 MHz and 250 MHz (Oversampling factor 2 is applied in the ADCs of the receivers). Further adjustment of the signal bandwidth can be done via oversampling of the discrete baseband signal. As mentioned in the deliverable D6.2 [16], the central controller software generates all transmit signal vectors and distributes them to the corresponding devices of the demonstrator platform via Ethernet. If the oversampling is done in the central controller software, a high oversampling factor (e.g. oversampling factor 8 with sampling clock frequency 320 MHz to achieve the 20 MHz for LTE signals) significantly increases the length of the signal vector (which scales with the oversampling factor). Very long signal vectors can result in much higher latency time of the distribution via Ethernet, causing the whole HIL-test to become inefficient. To solve this problem, the HIL-framework was improved, so that the oversampling is possible after the original signal vectors are distributed to each single device. With such "local oversampling" mechanism, the Ethernet is not the bottleneck of the HIL-test efficiency any more and the signal bandwidth can be flexibly adjusted.

For illustration, Fig. 4.2 shows a picture of the demonstrator platform under the channel emulator transmission mode. The configuration in this picture was for the spectrum sharing scenario SC2-TA, where two Tx antennas are used for each BS and one Rx antenna for each UT.

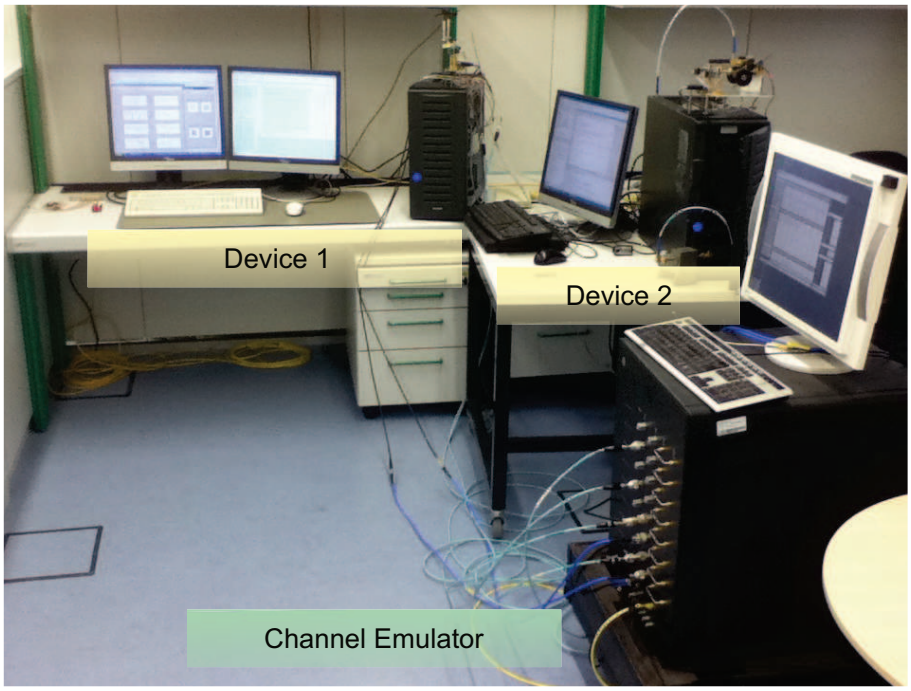

Figure 4.2: An example setup of the demonstrator platform under the channel emulator transmission mode. The spectrum sharing scenario SC2-TA was considered.

5 The Berlin LTE-Advanced Testbed

Except for HIL-demonstrator platform, a subset of the selected scenarios will be implemented on a further demonstrator platform i.e. the Berlin LTE-Advanced testbed provided by FhG. In this way, the visibility of the SAPHYRE project can be significantly improved towards the industry. In this chapter, the Berlin LTE-Advanced testbed is briefly described. Fig. 5.1 the setup of this testbed.

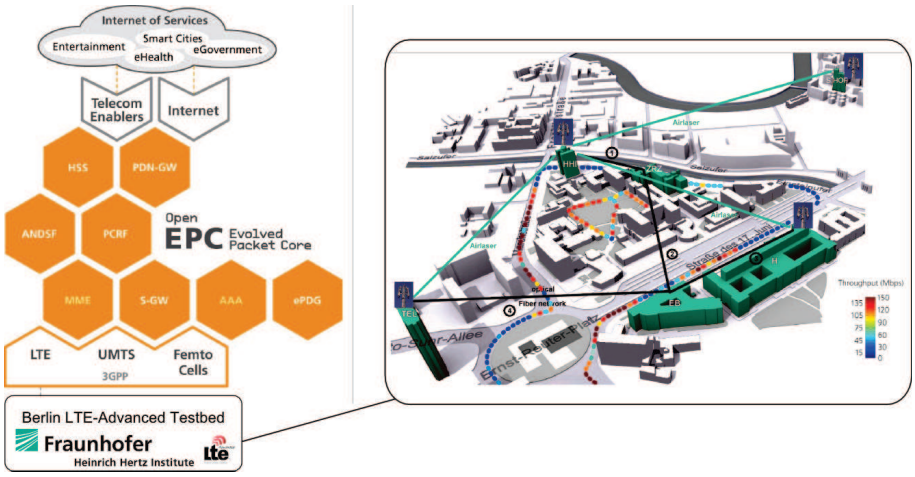

Figure 5.1: The Berlin LTE-Advanced testbed

The Berlin LTE-Advanced testbed serves for the early evaluation of 4G technologies with the focus on new LTE-Advanced concepts and their investigations in a realistic cellular environment. This testbed consists of a multi-cellular infrastructure with up to 9 base station sectors and is located in an urban macro environment in the center of Berlin. The testbed has multi-band support to operate in the 2.6 GHz UMTS extension band as well as in the 800 MHz digital dividend. It serves as demonstration platform for LTE-Advanced key technologies supporting mobility and end-to-end QoS concepts in an all-IP based cellular infrastructure. The LTE-Advanced Testbed serves for the early evaluation of LTE-Advanced concepts in a realistic cellular environment and for the demonstration of key technology features to increase spectral efficiency, range, throughput and quality-of-service.

Furthermore, the LTE-Advanced testbed features typical urban site deployments using commercial broadband antennas (700 MHz-2.7 GHz) with electrical down-tilt units connected to in-cabinet RF-frontends and/or remote radio heads using optical fiber links between all sites and the laboratory at Fraunhofer HHI. Furthermore, HHI can extend the current network infrastructure using radio based repeater/relay

modules flexible in bandwidth and frequency translation wireless backhauling to small micro and pico cells.

The LTE-Advanced Testbed has the unique inbuilt option of measuring multi-cell channels simultaneously and without crosswise interference due to a dedicated RS structure. The multi-cell deployment scenario can range from macro-only to overlays of macro-pico, macro-femto, macro-relays upto relays mounted on buildings, lamp posts or other types of infrastructure. Finally, this testbed allows both centralized and decentralized resource and interference management for wireless networks such as wireless cellular networks based on LTE/LTE-Advanced, cognitive radio networks and general mobile ad hoc networks. This includes novel cross-layer approaches, cooperative systems and heterogeneous management for QoS enhancement, energy efficiency and mobility robustness and QoS aware mobility.

While the HIL-demonstrator platform serves as verification of the SAPHYRE algorithms, the LTE-Advanced testbed makes a further step towards prototype design by taking the most relevant wireless standard into account.

6 Initial Implementation and Evaluation on the HIL-Demonstrator Platform

6.1 Scenario SC2-TA: Spectrum Sharing

6.1.1 Scenario and Test Case Description

6.1.1.1 Scenario Description

As shown in Fig. 6.1, this scenario consists of N_O BSs as well as N_O UTs of N_O different operators, where $N_O > 1$ (In Fig. 6.1, $N_O = 2$). Each BS and each UT can be equipped with multiple antennas. All operators share the same spectrum completely (at the same time) but have separate infrastructures.

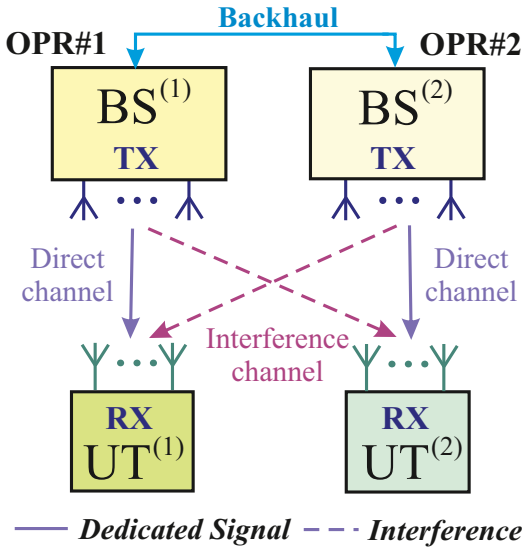

Figure 6.1: Scenario SC2-TA: Spectrum sharing without BS collocation.

By sharing the available frequency bands, the signal bandwidth of each operator can be significantly increased, leading to significant capacity enhancement. Moreover, to achieve a certain data rate, less transmission power is required. The reason is that according to the Shannon-Hartley theorem, capacity increases linearly with bandwidth but only logarithmically with Power. However, in the downlink, while each BS transmits data to the dedicated UT, it also generates interference to the UTs of the other operators. This also applies for the uplink. In order to suppress such

interference and to exploit the increased bandwidth, sophisticated coding/decoding and signal processing algorithms should be applied both in the BSs and the UTs. To allow the application of such resource sharing algorithms, the BSs of different operators are assumed to be able to cooperate with each other e.g. to exchange data like the related CSI. Such cooperation is done based on high capacity backhaul. Within this scenario, we should show that with spectrum sharing, higher performance e.g. the total throughput, can be achieved than the case without sharing.

6.1.1.2 Test Case Description

For the test of this scenario on the demonstrator platform, we restrict the investigation to the downlink. The number of operators as well as those of the BSs and UTs are set to 2. We assume 2 Tx antennas at each BSs and 1 Rx antenna at each UT. OFDM is applied as the PHY technique. The different BSs are assumed to be synchronized. Moreover, the transmitted signals are assumed to be OFDM signals. The total number of non-zero SubCarriers (SC) and NULL SCs can be flexible. The length of the Cyclic Prefix can also be flexible. Different channels can be used including Rayleigh channels, WINNER II channels [12] (channels generated from channel models that are obtained from realistic channel measurements) and measured LTE channels based on the LTE test field of FhG-HHI [11]. Different digital modulation waveforms can be applied e.g. BPSK, QPSK etc. We assume that no channel coding is applied. However, channel coding can be included in the future.

We will first test the algorithms in this scenario with Rayleigh channels and the measured LTE-channels for verification. In the case with Rayleigh channels, it is able to adjust the relations between the channel gains of the interference links and the direct links. For simplicity, we first investigate the case where the channel gains of the interference links are approximately equal to those of the direct links. Further test can be carried out for the cases where the channel gains of the interference links are significantly weaker or stronger than the direct links.

The following comparisons will be made:

- No spectrum sharing (each operator uses a half of the available frequency band) and with spectrum sharing: To show the SAPHYRE gain. In order to have fair comparison, BF techniques are also applied in the non-sharing case within the own band of each operator;

- In the case of sharing, different possible signal processing techniques (algorithms) are compared: To identify suitable algorithms.

The used performance metrics are: sum rate (in bits/s/Hz), single user rate (in bits/s/Hz), throughput (in bits/s/Hz).

6.1.2 Enabling Algorithms

Within the SAPHYRE project, a number of advanced BF techniques have been developed for this spectrum sharing scenario. A representative subset of them are selected and implemented on the demonstrator platform to provide proof-of-concept. These algorithms and some of the HIL results are also reported in [19] and [18]. In the following, the these BF techniques are briefly described and compared.

6.1.2.1 System Model

For the system model, subcarrier-wise description is used for both Transmitter (Tx)-Receiver (Rx) signal relation and BF algorithms. For simplicity, the subcarrier index is omitted. We assume each BS and UT have M_{T} and M_{U} Tx- and Rx antennas, respectively. The received data symbol at an arbitrary data subcarrier can be expressed as:

$$y_p = \sum_{q=1}^{2} \boldsymbol{g}_p^{\mathrm{T}} \boldsymbol{H}_{pq}^{\mathrm{T}} \boldsymbol{w}_q s_q + \boldsymbol{g}_p^{\mathrm{T}} \boldsymbol{\eta}_p, \tag{6.1}$$

where $p, q \in \{1, 2\}$ are the operator indexes and s_q is the Tx data symbol at the observed subcarrier of the q^{th} operator. $\boldsymbol{H}_{pq}$ is the $M_{\mathrm{T}} \times M_{\mathrm{U}}$ channel matrix between the q^{th} BS and the p^{th} UT. $\boldsymbol{g}_p$ and $\boldsymbol{w}_p$ are the decoding- and BF-vectors ($M_{\mathrm{U}} \times 1$ and $M_{\mathrm{T}} \times 1$) of the p^{th} operator, respectively, with $||\boldsymbol{w}_p||^2 \leq 1$ for Tx power constraint. Furthermore, $\boldsymbol{\eta}_p$ is the $M_{\mathrm{U}} \times 1$ noise vector, whose elements are Gaussian and have the variance σ_{n}^2. Finally, we assume that the BS obtains local Channel State Information (CSI), i.e. the channels between itself and the two UTs, via the UpLink (UL) and the backhaul.

6.1.2.2 Block-Diagonalization (BD) and Regularized Block-Diagonalization (RBD)

The original BD [28] or RBD [29] has been developed to suppress the inter-user interference in the downlink of multi-user MIMO systems. Now, they are extended to the scenario of inter-operator spectrum sharing. First, (6.1) is rewritten as follows

$$\begin{bmatrix} y_1 \\ y_2 \end{bmatrix} = \underbrace{\begin{bmatrix} \boldsymbol{g}_1^{\mathrm{T}} \boldsymbol{H}_{11}^{\mathrm{T}} \boldsymbol{w}_1 & \boldsymbol{g}_1^{\mathrm{T}} \boldsymbol{H}_{12}^{\mathrm{T}} \boldsymbol{w}_2 \\ \boldsymbol{g}_2^{\mathrm{T}} \boldsymbol{H}_{21}^{\mathrm{T}} \boldsymbol{w}_1 & \boldsymbol{g}_2^{\mathrm{T}} \boldsymbol{H}_{22}^{\mathrm{T}} \boldsymbol{w}_2 \end{bmatrix}}_{\boldsymbol{H}_e} \begin{bmatrix} s_1 \\ s_2 \end{bmatrix} + \begin{bmatrix} \boldsymbol{g}_1^{\mathrm{T}} \boldsymbol{\eta}_1 \\ \boldsymbol{g}_2^{\mathrm{T}} \boldsymbol{\eta}_2 \end{bmatrix},$$

where the off-diagonal elements in $\boldsymbol{H}_e$ represent Inter-operator Interference (IOI), which should be completely removed by BD. Such IOI removal requires to extract the null space of the interference channel, which can be done with the following singular value decomposition (SVD): $\boldsymbol{H}_{pq}^{\mathrm{T}} = \boldsymbol{U}_{pq} \cdot \boldsymbol{\Sigma}_{pq} \cdot \boldsymbol{V}_{pq}^{\mathrm{H}}, \forall p \neq q$. The null space of $\boldsymbol{H}_{pq}^{\mathrm{T}}$, denoted as $\boldsymbol{V}_{pq}^{(0)}$, consists of the last $(M_{\mathrm{T}} - r_{pq})$ rows of $\boldsymbol{V}_{pq}$, where r_{pq}

indicates the rank of $\boldsymbol{H}_{pq}^{\mathrm{T}}$. After zero-forcing the IOI, the SVD of the effective channel for the q^{th} operator is written as $\bar{\boldsymbol{H}}_{qq}^{\mathrm{T}} = \boldsymbol{H}_{qq}^{\mathrm{T}}\boldsymbol{V}_{pq}^{(0)} = \boldsymbol{U}_{qq} \cdot \boldsymbol{\Sigma}_{qq} \cdot \boldsymbol{V}_{qq}^{\mathrm{H}}, \forall p \neq q$. Let $\boldsymbol{V}_{qq}^{(1)}$ be a submatrix consisting the first r_{qq} rows of $\boldsymbol{V}_{qq}$, where r_{qq} indicates the rank of $\bar{\boldsymbol{H}}_{qq}^{\mathrm{T}}$. The columns of $\boldsymbol{V}_{qq}^{(1)\mathrm{H}}$ span the signal space of $\boldsymbol{H}_{qq}^{\mathrm{T}}$ projected into the null space of $\boldsymbol{H}_{pq}^{\mathrm{T}}$. In order to maximize the sum rate of the q^{th} operator, the BF vector is obtained as $\boldsymbol{w}_q = \boldsymbol{V}_{pq}^{(0)}\boldsymbol{v}_{qq}^{(1)}$, where $\boldsymbol{v}_{qq}^{(1)}$ is the first column of $\boldsymbol{V}_{qq}^{(1)\mathrm{H}}$. The received filter $\boldsymbol{g}_q$ is derived as $\boldsymbol{g}_q = \boldsymbol{u}_{qq}^{(1)}$ with $\boldsymbol{u}_{qq}^{(1)}$ denoting the left dominant singular vector of $\bar{\boldsymbol{H}}_{qq}^{\mathrm{T}}$.

Instead of zero-forcing the IOI, RBD is designed to maximize the system sum rate under the constraint that the Frobenius norm of the IOI plus noise is minimized. The BF vectors of RBD are expressed as $\boldsymbol{w}_q = \beta\boldsymbol{W}_{q,a}\boldsymbol{w}_{q,b}$, where $\boldsymbol{W}_{q,a}$ and $\boldsymbol{w}_{q,b}$ are used for IOI suppression and rate optimization, respectively. Additionally, we have a scalar β to fulfill the Tx power constraint. Assuming $||\boldsymbol{w}_{q,b}|| = 1$ and full-power transmission, we have $\beta^2||\boldsymbol{W}_{q,a}\boldsymbol{w}_{q,b}||^2 = \beta^2||\boldsymbol{W}_{q,a}||_F^2 = P_{\mathrm{T}}$, with P_{T} the Tx power. Therefore, we choose $\beta = \sqrt{P_{\mathrm{T}}}/||\boldsymbol{W}_{q,a}||_F$. The matrix $\boldsymbol{W}_{q,a}$ is designed to minimize the Frobenius norm of the IOI plus noise, i.e., $\boldsymbol{W}_{q,a} = \min_{\boldsymbol{W}_{q,a}} E\{||\boldsymbol{H}_{pq}^{\mathrm{T}}\boldsymbol{W}_{q,a}||_F^2 + \frac{||\boldsymbol{\eta}_p||_2^2}{\beta^2}\},, \forall p \neq q$. After computing the SVD of the interference channel $\boldsymbol{H}_{pq}^{\mathrm{T}} = \boldsymbol{U}_{pq} \cdot \boldsymbol{\Sigma}_{pq} \cdot \boldsymbol{V}_{pq}^{\mathrm{H}}$, we get $\boldsymbol{W}_{q,a} = \boldsymbol{M}_{q,a}\boldsymbol{D}_{q,a}$, where $\boldsymbol{M}_{q,a} = \boldsymbol{V}_{pq}$ and $\boldsymbol{D}_{q,a} = (\boldsymbol{\Sigma}_{pq}^{\mathrm{T}}\boldsymbol{\Sigma}_{pq} + \frac{M_{\mathrm{U}}\sigma_n^2}{P_{\mathrm{T}}}\boldsymbol{I}_{M_{\mathrm{T}}})^{-\frac{1}{2}}$ is a diagonal power loading matrix. The matrix $\boldsymbol{D}_{q,a}$ is positive definite in order to get a nontrivial solution of $\boldsymbol{W}_{q,a}$. Similarly to BD, the effective channel after IOI suppression is written as $\bar{\boldsymbol{H}}_{qq}^{\mathrm{T}} = \boldsymbol{H}_{qq}^{\mathrm{T}}\boldsymbol{W}_{q,a} = \boldsymbol{U}_{qq} \cdot \boldsymbol{\Sigma}_{qq} \cdot \boldsymbol{V}_{qq}^{\mathrm{H}}$. The vector $\boldsymbol{w}_{q,b}$ is obtained as $\boldsymbol{w}_{q,b} = \boldsymbol{v}_{qq}^{(1)}$ to enhance the sum rate for the q^{th} operator, where $\boldsymbol{v}_{qq}^{(1)}$ is the right dominant singular vector of $\bar{\boldsymbol{H}}_{qq}^{\mathrm{T}}$. The received filter $\boldsymbol{g}_q$ is derived as the left dominant singular vector of $\bar{\boldsymbol{H}}_{qq}^{\mathrm{T}}$.

6.1.2.3 Game Theoretic BF Techniques

For simplicity, we assume $M_{\mathrm{U}} = 1$ for the game theoretic BF-techniques. Accordingly, $\boldsymbol{H}_{pq}$ becomes a $M_{\mathrm{T}} \times 1$ vector. Moreover, $\boldsymbol{g}_{1;2}$ becomes a scalar.

6.1.2.4 SINR Region and Efficient Transmission

The Signal to Interference plus Noise Ratio (SINR) at UT p is

$$\phi_p(\boldsymbol{w}_1, \boldsymbol{w}_2) = \frac{|\boldsymbol{H}_{pp}^{\mathrm{T}}\boldsymbol{w}_p|^2}{|\boldsymbol{H}_{pq}^{\mathrm{T}}\boldsymbol{w}_q|^2 + \sigma_{\mathrm{n}}^2}, \quad p \neq q. \tag{6.2}$$

This results in the achievable rate $\log_2(1+\phi_p(\boldsymbol{w}_1, \boldsymbol{w}_2))$. The *SINR region* is the set of all achievable SINR tuples defined as $\Phi := \{(\phi_1(\boldsymbol{w}_1, \boldsymbol{w}_2), \phi_2(\boldsymbol{w}_1, \boldsymbol{w}_2)) : \|\boldsymbol{w}_p\|^2 \leq 1\}$. In the SINR region, tuples can be ranked according to their Pareto efficiency. An SINR tuple $(\phi_1', \phi_2') \in \Phi$ is *Pareto superior* to $(\phi_1, \phi_2) \in \Phi$ if $(\phi_1', \phi_2') \geq (\phi_1, \phi_2)$,

where the inequality is component-wise and strict for at least one component. The transition from (ϕ_1, ϕ_2) to (ϕ_1', ϕ_2') is called a *Pareto improvement*. Situations where Pareto improvements are not possible are called *Pareto optimal*.

The set of BF vectors that are relevant for Pareto optimal operation are parameterized by a single real-valued parameter λ_p for each BS $p \neq q$ as [8, Corollary 1]

$$\boldsymbol{w}_p(\lambda_p) = \sqrt{\lambda_p}\frac{\boldsymbol{\Pi}_{\boldsymbol{H}_{pq}}\boldsymbol{H}_{pp}}{\|\boldsymbol{\Pi}_{\boldsymbol{H}_{pq}}\boldsymbol{H}_{pp}\|} + \sqrt{1-\lambda_p}\frac{\boldsymbol{\Pi}^{\perp}_{\boldsymbol{H}_{pq}}\boldsymbol{H}_{pp}}{\|\boldsymbol{\Pi}^{\perp}_{\boldsymbol{H}_{pq}}\boldsymbol{H}_{pp}\|}. \tag{6.3}$$

with $\lambda_p \in [0, \lambda_p^{\mathrm{MRT}}]$, $\lambda_p^{\mathrm{MRT}} = \|\boldsymbol{\Pi}_{\boldsymbol{H}_{pq}}\boldsymbol{H}_{pp}\|^2/\|\boldsymbol{H}_{pp}\|^2$. The set of BF vectors in (6.3) includes Maximum Ratio Transmission (MRT) ($\lambda_p = \lambda_p^{\mathrm{MRT}}$) and ZF ($\lambda_p = \lambda_p^{\mathrm{ZF}} = 0$). This parametrization in (6.3) is valuable for designing efficient low complexity distributed resource allocation schemes such as the algorithms described next in Sec. 6.1.2.5 and Sec. 6.1.2.6.

The SINR of the p^{th} UT in terms of the parameters in (6.3) is [21]

$$\phi_p(\lambda_1, \lambda_2) = \frac{\left(\sqrt{\lambda_p g_p} + \sqrt{(1-\lambda_p)\check{g}_p}\right)^2}{\sigma_{\mathrm{n}}^2 + \lambda_q g_{qp}}, \quad q \neq p. \tag{6.4}$$

where $\lambda_p \in [0, \lambda_p^{\mathrm{MRT}}]$ and $g_p := \|\boldsymbol{\Pi}_{\boldsymbol{H}_{pq}}\boldsymbol{H}_{pp}\|^2$, $\check{g}_p := \|\boldsymbol{\Pi}^{\perp}_{\boldsymbol{H}_{pq}}\boldsymbol{H}_{pp}\|^2$, $g_{pq} := \|\boldsymbol{H}_{pq}\|^2$, $p \neq q$. It can be observed in (6.4) that the interference term $\lambda_q g_{qp}$ scales linearly with λ_q. Accordingly, the parameter λ_q can be interpreted as a scaling of interference at the counter Rx. A reduction in λ_q increases the SINR of the p^{th} UT for fixed λ_p.

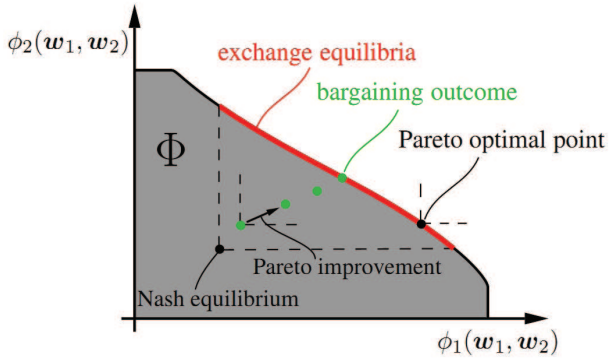

Figure 6.2: An illustration of an SINR region.

In the following, two game theoretic BF techniques are presented. Both techniques are iterative, with the maximum iteration number as a design parameter. Both techniques allow Pareto improvement at each iteration. The objectives of both algorithms are not sum rate maximization but that the outcome is a Pareto improvement of the Nash Equilibrium (NE).

6.1.2.5 Cooperative BarGaining (CoBG) Algorithm

In this section, we shortly describe the CoBG algorithm [24] utilizing the SINR region illustration in Fig. 6.2. A special operating point in this region is the NE, which is the solution of a strategic game [7, Chapter 7.1] between the links i.e. an operating point with noncooperative links. In our BF setting, the NE corresponds to joint MRT [13] which is in general not Pareto optimal as illustrated in Fig. 6.2. Of interest is to improve the joint performance of the links from the NE outcome. All Pareto optimal points which dominate the NE in the SINR region are specified in Fig. 6.2 as *exchange equilibria*. These equilibria are outcomes of an exchange economy [7, Chapter 5.1] between the links and are characterized in [21] in closed form. In order to reach any exchange equilibrium, an exchange process needs to be formulated. This process starts at the NE and terminates at an exchange equilibrium. In [24], such a process is constructed. The idea behind the mechanism is to interpret the parameters for the BF vectors in (6.3) as goods which the links *bargain* over. The links exchange the amounts of goods within themselves in such a way that Pareto improvements are achieved in each bargaining stage. The main tool that aids in the analysis for the choice of the cooperative BF vectors is the preference representation of the links in the Edgeworth box. In the Edgeworth box, the *exchange lens* contains all distributions of the goods between the links which lead to Pareto improvements in the SINR region. In [24], the proposals of the links in each bargaining step are systematically studied and chosen such that Pareto improvements are achieved. The bargaining process requires four bits of signaling between the BSs in each bargaining step. In Fig. 6.2, the green circles illustrate the outcomes of the bargaining stages which start at the NE and end at an exchange equilibrium.

6.1.2.6 Cooperative Beam-Forming (CoBF) Algorithm

The CoBF algorithm has been reported in [15] in detail. It uses IOI as bargaining value and works with both instantaneous and statistical CSI. With CoBF, cooperation among the BSs is enabled, which can increase both users' rates by lowering the overall IOI. First, NE is used as a starting point (i.e. BF with MRT) [13]. Among the operating points that might *potentially* be Pareto-optimal, this is the one with the highest IOI (see Sec. 6.1.2.4). At each iteration, the maximum tolerated IOI is lowered. Under this constraint, the useful power over the direct channel is maximized. When the maximum IOI decreases, the maximum useful power decreases as well. However, up to a certain point, the SINR (6.2) will increase. After computing the BF vectors at each iteration, rate estimation is carried out to check whether the rate is increased or decreased. This iteration procedure is proceeded as long as both rates increase. The core optimization problem is solved in closed form by utilizing the parameterization (6.3) - the optimum solution is the solution of a quadratic equation. When the algorithm converges, a nearly Pareto-optimal operating point

is reached.

Compared to CoBG, CoBF can also start with ZF BF at all BSs [13]. This starting point is chosen when both links get higher rates at the ZF point than at the NE. If the algorithm starts at ZF, the maximum tolerable IOI is increased in each iteration. The corresponding motivation is that the ZF points might be closer to the Pareto boundary than the NE point. This is especially true for high SNR.

6.1.2.7 Comparison of the Proposed BF Techniques

Both BD and RBD are closed-form solutions, while both CoBG and CoBF are iterative algorithms. Thus, the computational complexities of BD and RBD are generally much lower than those of CoBG and CoBF. Compared to BD, RBD improves the system sum rate performance at low SNRs since it can balance the IOI with noise enhancement. At high SNRs, the performance of RBD converges to BD. While CoBG and CoBF only works for $M_{\mathrm{U}} = 1$, BD and RBD work for any antenna configuration satisfying $M_{\mathrm{T}} > M_{\mathrm{U}}$. However, as will be shown in Sec. 6.1.5, CoBG and CoBF generally have better performance than BD and RBD. Compared to CoBF, the CoBG solution can be more closer to the Pareto optimal point. However, CoBG generally requires a larger iteration number than CoBF for convergence and has higher complexity and overhead.

6.1.3 Practical Implementation Issues

The proposed BF techniques have been implemented on the demonstrator platform with $M_{\mathrm{T}} = 2$ and $M_{\mathrm{U}} = 1$. The mapping of the scenario is shown in Fig. 6.6. During the implementation, several practical implementation problems have been identified, which are very relevant for the practical deployment of these algorithms. To solve these problems, corresponding solutions have been developed and implemented.

6.1.3.1 Channel Variation and Time Synchronization Error (TSE)

Before the BF vectors are computed using the proposed algorithms, channel estimation has to be carried out, which can be done by extending standard MIMO channel estimation schemes[1]. However, when the computed BF vectors are applied for signal transmission, the channel may have already changed, e.g. due to mobility. Even if the channel has not changed, TSE may occur, which causes subcarrier-dependent phase error in the Rx data symbols[2]. Actually, the effect of TSE can be regarded as a special case of channel variation. The most simple and

[1] These channel estimates have to be fedback from UTs to BSs via the UL. In the HIL platform, the UL is replaced by an Ethernet connection for simplicity.

[2] Assuming the time synchronization error is within the tolerable range of the Cyclic Prefix (CP).

effective way to cope with this problem is to carry out additional equalization of the residual channel effect, which can be estimated using either the pilot subcarriers or additional preambles. Note that such additional equalization also helps to compensate the Common Phase Error (CPE) caused by Carrier Frequency Offset (CFO). However, this simple method is only suitable for low mobility cases. For high mobility, more advanced solution e.g. channel prediction has to be applied.

In the implementation, we have added one more pilot OFDM symbol at the beginning of each frame, which is also precoded for BF. At the receiver, this pilot OFDM is used to estimate the effective channel after BF (using MLE or MMSE estimation). Afterwards, the data OFDM symbols are equalized using the estimated effective channel coefficients.

6.1.3.2 Rate Estimation and Distributed BF Vector Computation

Both game theoretic BF techniques in Sec. 6.1.2.3 require rate estimation at each iteration. One approach is to send pilot sequences at each iteration and get feedbacks from the UTs. At the early implementation stage of these two algorithms, such rate estimation mechanism has been implemented and integrated to the demonstrator platform. The pilot sequence consists of a number of OFDM symbols with known data. In each iteration, these OFDM symbols (of all BSs) are precoded with the temporary BF vectors and transmitted to the UTs. Each UT measures the SINR of these received OFDM symbols based on their prior knowledge and calculate whether the rate is increased or decreased compared to the last iteration. The rate increment information is fed back to the BSs for the calculation of the BF vectors in the next iteration. Fig. 6.3 and Fig. 6.4 show the estimated rates of a HIL-test at different subcarriers and different UTs at each iteration. As shown, the CoBG algorithm requires a much larger number of iterations than the CoBF algorithm. Furthermore, we can notice that despite the general increasing tendency with increasing iteration number, the final rate does not necessarily converge to the highest one. After joint analysis with WP3, we have identified that the problem is the estimation error of the rates, which results from the channel estimation error and noise power variation. Thus, the approach of sending pilot sequence is probably not suitable.

A further disadvantage of the pilot based rate estimation is that it leads to very high communication overhead. It also results in long test time of the HIL-test. Moreover, the channels may have changed significantly during the iterative computation of the BF vectors, resulting in performance degradation.

As a solution, we have proposed a much advantageous approach, which computes the rate directly from the CSI and the noise power estimates. This approach requires much less overhead. However, if each BS only has local CSI, they can not estimate all rates on their own. In [24], the two BSs are supposed to exchange the rate change information at each iteration e.g. via the backhaul. Such exchange can significantly increase the time for BF vector computation (assuming N_I iterations,

N_I information exchange sessions via the backhaul are required). A more efficient implementation is that the BSs exchange all CSI and the noise power estimates before computing the BF vectors. Afterwards, identical BF vector computation is carried out in parallel in both BSs, which will yield the same outcomes. In other words, all BSs play the same game internals and will come to the same outcome. In this way, the processing time for BF vector computation is minimized.

Note that unlike CoBG and CoBF, BD and RBD require only the local CSI and the noise estimates for BF vector computation.

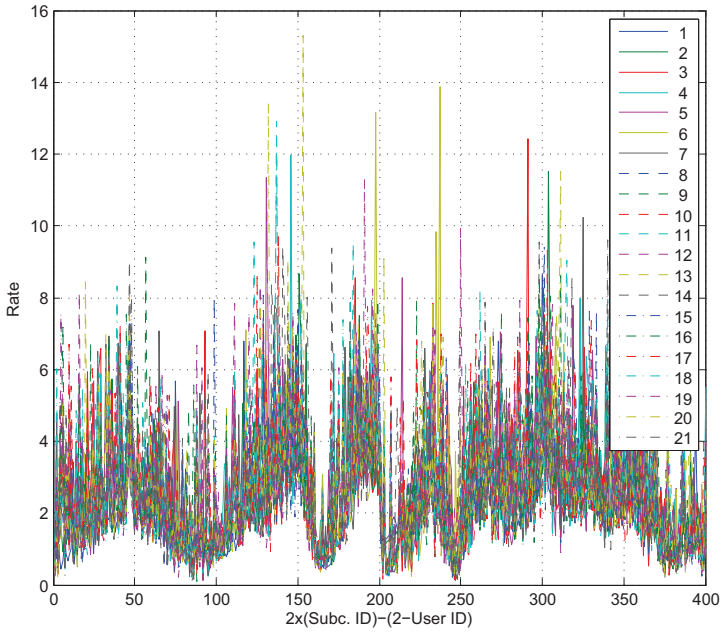

Figure 6.3: The rate evolution of the CoBG algorithm for different iterations.

6.1.3.3 Colored Noise

Except for BD, the proposed BF algorithms require knowledge about the noise power[3]. In most of the theoretical works, the noise is assumed to be white, which is not true in the practice. Due to the analog Low-Pass Filters (LPF) at the Rx and the spurious spectral components, the noise is generally colored and contains narrow band interference, as shown in Fig. 6.5. Moreover, the noise power of different UTs is different. Thus, separate subcarrier-wise noise power estimation has to be carried out at each UT. The simplest method is to take Discrete Fourier Transform (DFT) on the noise sequences at the individual UTs. Moreover, the original algorithms designed for white noise with identical variance for all UTs have to be modified so

[3]For regularization in RBD and for rate estimation in CoBG and CoBF.

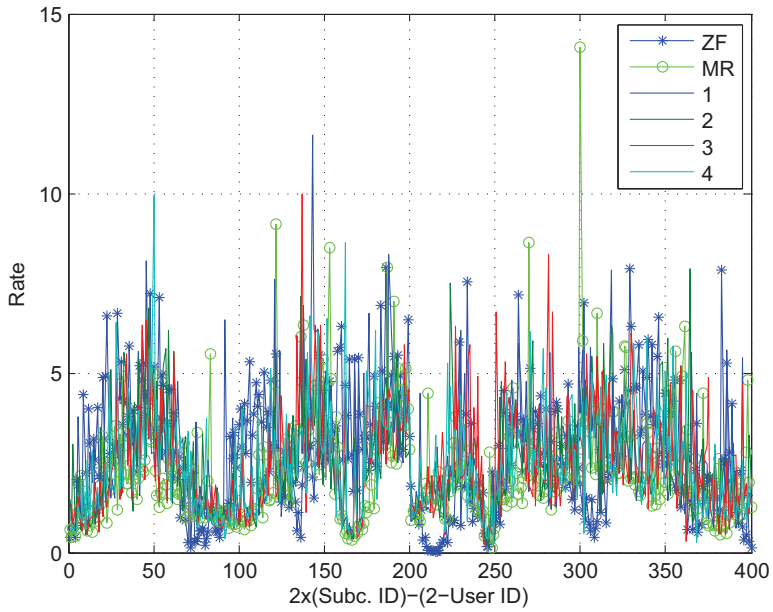

Figure 6.4: The rate evolution of the CoBF algorithm for different iterations.

that they also work in the cases that different UTs have different noise power levels. Note that such modification and improvement corresponds to the sixth step of the scenario implementation work flow in Ch. 3.

6.1.3.4 Signal Amplitude Scaling for Digital-to-Analog Converter (DAC)

Usually, the amplitude of the digital Tx signals have to be properly scaled before they are fed to the DACs, so that on the one hand, the signals are not clipped to much and on the other hand, the quantization error is as low as possible. Since maximum peak amplitude of different signal frames can have large difference, direct scaling based on the maximum peak amplitude of each signal frame will lead to considerable fluctuation of the signal power (if the Tx attenuation is not adjusted adaptively). To allow quasi stable output signal power of the DACs, a fixed power backoff factor should be defined (w.r.t. the maximum DAC input amplitude without clipping). By adjusting this backoff factor, certain clipping of the digital signal is allowed, but a tradeoff between DAC-clipping and quantization error can be achieved.

When BF is applied, this scaling factors should be identical for all Tx antennas of a BS. Furthermore, except for BD, the scaling factors of the different BSs should also be identical. Otherwise, performance degradation is expected (assuming that a global scaling factor is used for channel estimation). Depending on the channel

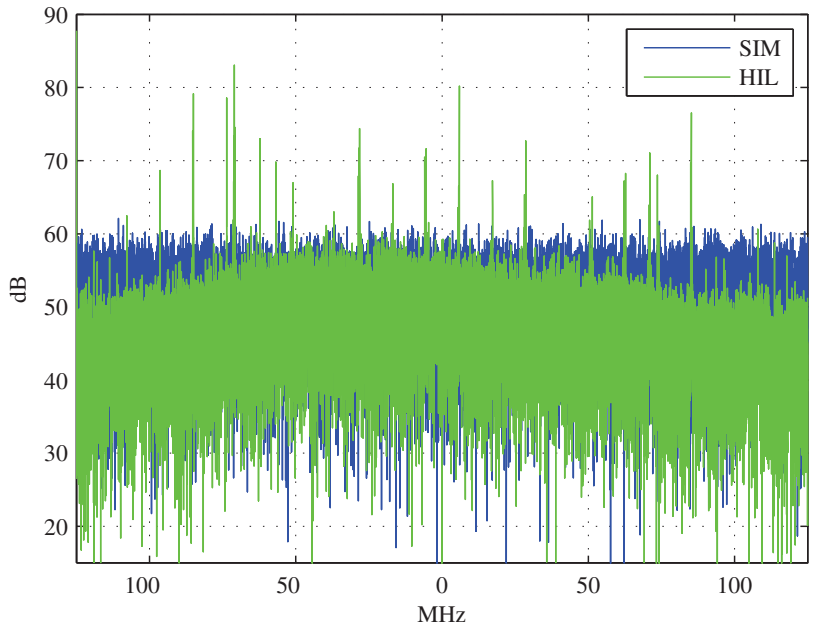

Figure 6.5: The spectra of the noise on the demonstrator platform (denoted as "HIL") as well as an ideal AWGN (denoted as "SIM").

realization, the BF can change the signal power distribution between Tx antennas from one signal frame to another (assuming constant sum power of all Tx antennas at each BS). Thus, this global scaling factor has to be recomputed for every signal frame. This global scaling factor should be computed based on the predefined backoff value and the power of all precoded signal branches (at the DAC inputs). Furthermore, this power information has to be exchanged between both BSs, so that they can find out the global scaling factor.

6.1.3.5 Rescaling of the Channel Coefficients or the Noise Power

For most of the algorithms, the estimation of noise power (subcarrier-wise) is required (e.g. RBD, CoBG and CoBF). Actually, for these algorithms, the relation between the channel gain and the noise power is most important, instead of the absolute value of the noise power. For the application of BF techniques, the channel estimation and the precoded signal transmission based on the estimated channels have to be carried out in different communication signal frames[4]. These different signal frames may have different amplitude scaling factors for the DAC. The change of the amplitude scaling factor actually results in the change of the effective chan-

[4]Typically, if the channel estimation is done within the n-th communication signal frame, the corresponding precoded transmission using these channel estimates will be in the $(n+1)$-th communication signal frame.

nel[5]. Thus, before the BF vectors are calculated, either the channel estimates or the noise power has to be rescaled, so that their relation fits the actual value. However, at the moment of the BF vector calculation, the amplitude scaling factor (for the DACs) of the current signal frame is still unknown, since it in turns depends on the BF vectors[6]. To solve this "deadlock" problem, two methods can be applied. The first one is to predefine a fixed amplitude scaling factor, which is used both to rescale the channel coefficients and to scale the transmit signals. This predefined value can be chosen according to previous transmissions. However, with such a predefined amplitude scaling factor, the DAC-backoff can not be kept constant any more. Moreover, the clipping by the DAC is not controlled systematically. A more advanced method is iterative computation, which requires higher computational complexity. First, an initial value of the amplitude scaling factor is set, probably by taking the value from the last frame. Afterwards, this value is used to rescale the channel estimates or noise power and then to calculate the temporary BF vectors. After the temporary BF vectors are available, the corresponding amplitude scaling factor can be computed. This value is used again for the calculation of the BF vectors in the next iteration. After several iterations, the amplitude scaling factor will converge. Simulation results show that usually, three iterations are sufficient for such convergence.

6.1.4 Mapping on the HIL-Demonstrator Platform

In the deliverable D6.1a [20], the initial implementation results of this scenario was reported, which was based on the mapping of this scenario to the RF cable network mode of the demonstrator platform (using multi-stage transmission mapping technique). During the second period of the SAPHYRE project, the implementation was extended and mapped to the channel emulator mode, which is shown in Fig. 6.6. As shown, two experimental devices are used. While each transmitter of both device acts the role of the BS, the receiver of one device acts the roles of both UTs. Furthermore, one device acts as the master (w.r.t. trigger signal distribution etc.), while the other one acts as the slave. All transmitter outputs are connected to inputs of the Elektrobit F8 channel emulator, while the receiver inputs corresponding to the UTs are connected to the output of the channel emulator. The picture of the corresponding setup on the demonstrator platform was already shown in Fig. 4.2.

Fig. 6.7 shows the flowchart of the HIL test program. First, general parameter settings are carried out. Afterwards, the channel set up is carried out including the activation of the channel emulator mode, the connection establishment with the channel emulator (for remote control), the loading of the channel emulator file and the starting of the channel emulation. Afterwards, channel realization control and channel estimation (and noise power estimation) are carried out. With

[5] In practice, the amplitude scaling also counts as the channel effect.

[6] The BF vectors have influence both on the signal amplitude characteristic and on the signal power distribution between Tx antennas.

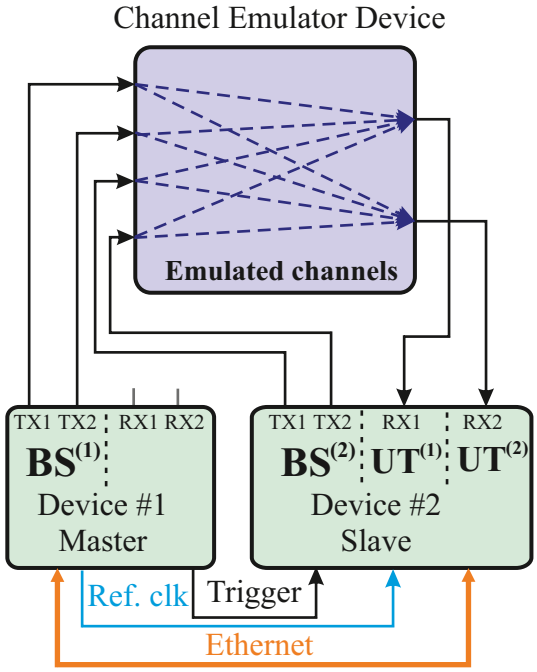

Figure 6.6: Mapping of SC2-TA on the HIL platform with the channel emulator mode.

each channel realization, different SNR levels are applied by adjusting the variable gain amplifiers at the modulators. For each channel realization and each SNR level, signal transmissions with both non-sharing and sharing are carried out. In the sharing case, different BF algorithms are applied. During each transmission, some intermediate results e.g. the received signal constellation and the currently measured throughput can be shown. After all transmissions are finished, the results will be evaluated and saved.

6.1.5 Initial HIL-Test Results

In the HIL test, OFDM signals with 2048 subcarriers and CP length of 144 samples were transmitted, which comply with the LTE standard. The transmission signal bandwidth was 20 MHz. Moreover, the measured LTE channels reported in [11] were used (i.e. loaded in the channel emulator). The scenario (setup) of the channel measurement is shown in Fig. 6.8. The distance between the two BSs were 540 meter, while that between the two UTs is 25 meter. Moreover, both UTs are about 485 meters away from the corresponding BS. This scenario of the channel measurement is very typical for the considered spectrum sharing scenario. For simplicity, the channel realization for each signal frame was kept constant i.e. the "stepping" mode of the channel emulator was used (see Sec. 4.2). Fig. 6.9 shows the estimated channel frequency response of the LTE channels including the influence of the RF

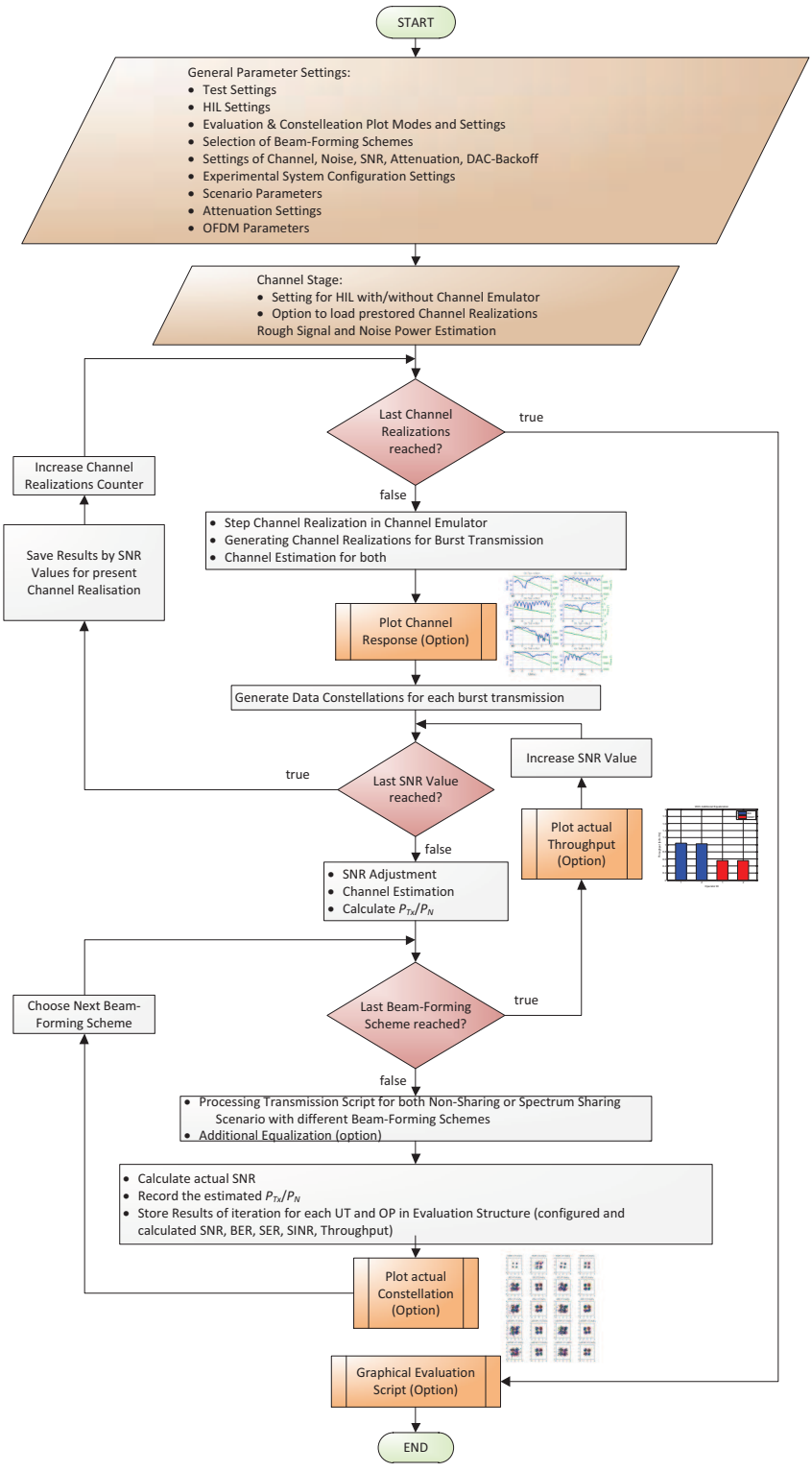

Figure 6.7: Flowchart of the software implementation of the spectrum sharing scenario.

chains.

In the non-sharing case, each operator transmits in half of the available spectrum using Eigen-Mode Beam-Forming (EMBF) or the so called MRT[7]. This allows the comparison between the non-sharing and the sharing cases to be fare. In the sharing case, the proposed advanced BF algorithms including BD, RBD, CoBG and CoBF are applied.

Fig. 6.10 shows the measured received signal constellation (with QPSK) with different BF algorithms as well as in the non-sharing case. Both the cases with and without additional Rx equalization are shown. As can be seen, due to interference, the constellations in the sharing cases are generally more noisy than that in the non-sharing case. But as will be shown later, the benefit of the sharing comes from the doubled bandwidth. We can also seen that the additional equalization can correct the slight phase rotations of the constellations, but it can also cause further distortion due to estimation error of the equivalent channel. Thus, the additional equalization algorithm still needs improvement.

Fig. 6.10 shows the instantaneous measured throughput of the different cases. The normalized Tx power to Noise power Ratio (TNR, normalized to the case with 0 dB channel gain) was about 16 dB. As shown, the sharing cases have much higher throughput than the non-sharing case. However, since no adaptive modulation and coding was applied, this comparison is still not completely fair. More fair comparison is found in the following capacity diagrams, where the capacity is calculated based on the measured SINR of the received signal constellations.

Fig. 6.12 shows the measured sum capacity as a function of TNR. Only the cases without additional equalization are shown, since with the channel emulator, consistent time synchronization can be achieved. The per user capacity is shown in Fig. 6.13 as reference. As shown, with sufficient TNR, the capacity with sharing is much higher than without sharing. Thus, the sharing gain can be verified in the first place. Furthermore, among the proposed BF algorithms, the game theoretic algorithms generally outperform BD and RBD. The major performance difference between both algorithms classes lies in the low TNR region. With high TNR, the performance of all algorithms converges.

Interestingly, we found out that among these algorithms, the higher the complexity, the better the performance. As mentioned in Sec. 6.1.2.7, the CoBG has the highest computational complexity. In the HIL test, CoBG also has the best performance. In contrast, BD has the lowest computational complexity but is outperformed by all the other algorithms.

We also notice that performance gain of the other BF algorithms over BD is not very large. However, in the pre-simulation results, we found out that with much weaker interference links, the performance enhancements by CoBG and CoBF compared

[7]We assume identical averaged sum Tx-power per subcarrier in all cases.

to BD and RBD can be larger. The corresponding HIL verification remains future work.

Finally, we can conclude that the choice of the BF algorithm depends on the targeted performance, the operating SNR region and the computational capacity of the BSs.

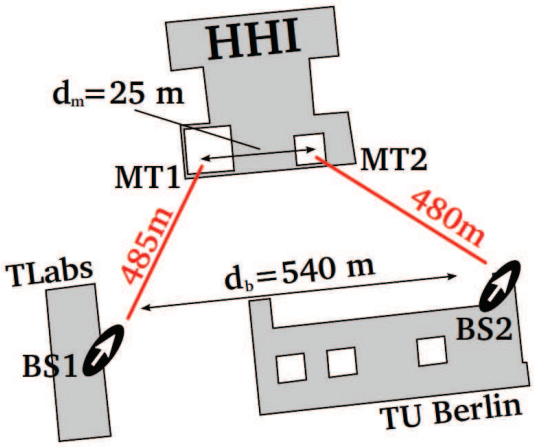

Figure 6.8: The setup for the measurement of the LTE channels.

6.1.6 Future Works

In the future, we will proceed testing this scenario with different channel parameterizations. We plan to generate Rayleigh channels in the channel emulators with certain channel gain relations between the interference links and the direct links, so that we can test the behavior of the different algorithms depending on such channel gain relations. At the same time, we expect new algorithms to be integrated e.g. the sum-rate maximization based BF technique developed by FhG.

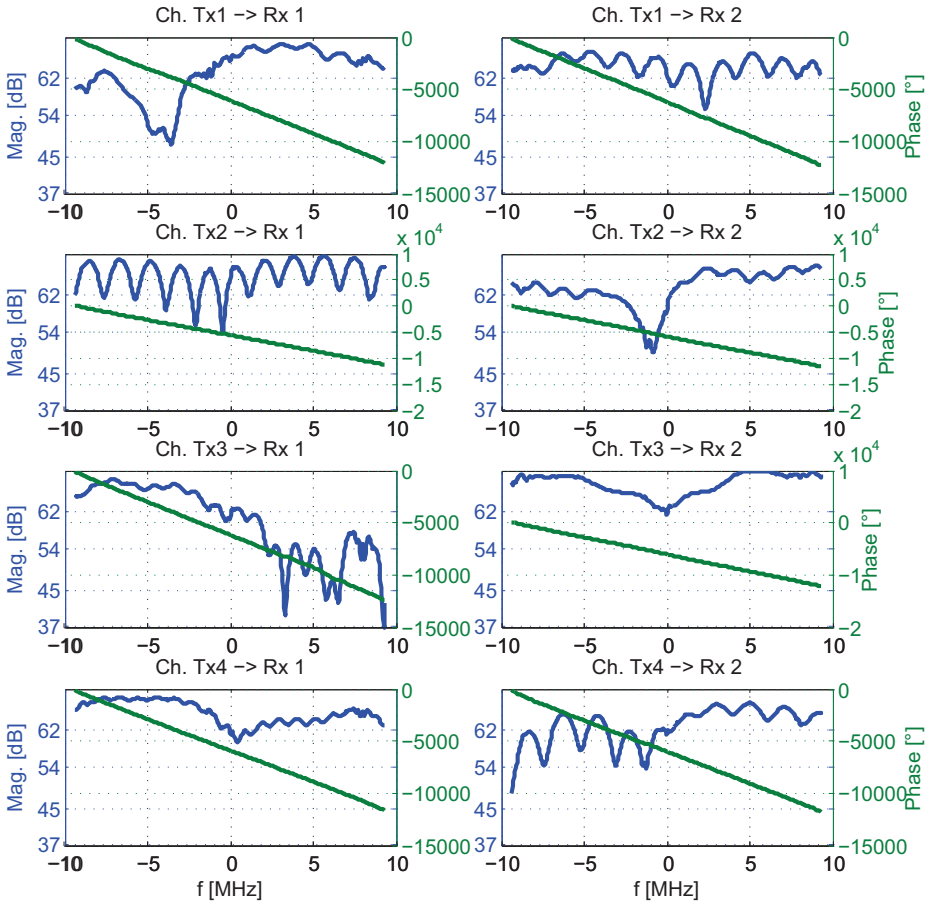

Figure 6.9: Frequency response of the measured LTE channels.

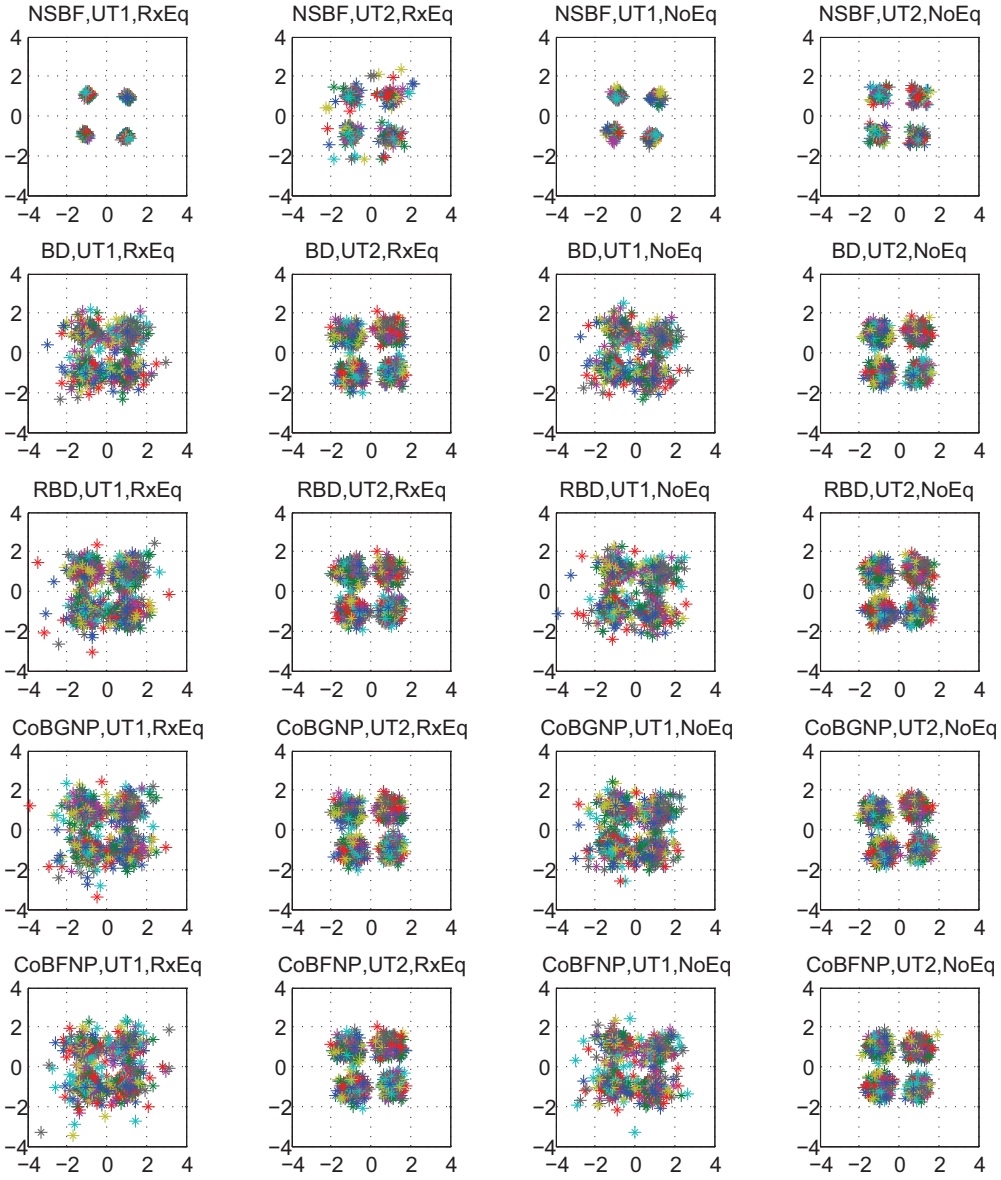

Figure 6.10: Measured received signal constellation with different BF algorithms as well as in the non-sharing case. Both the cases with and without additional Rx equalization are shown.

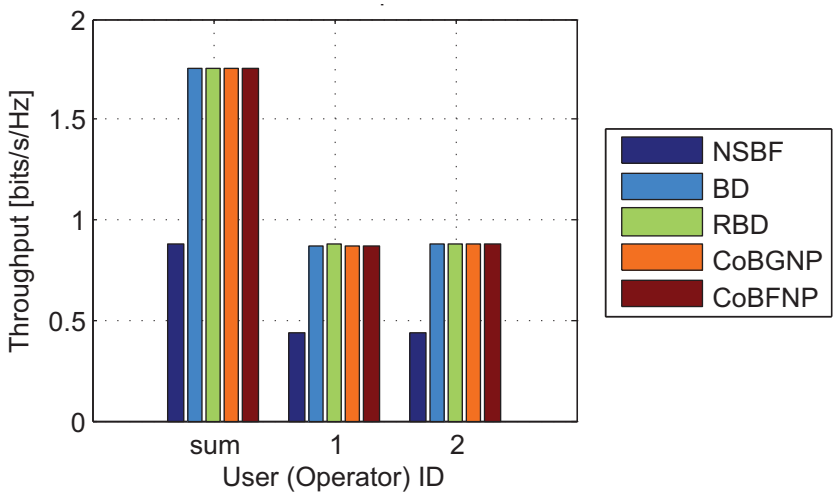

Figure 6.11: Measured throughput with different BF algorithms as well as in the non-sharing case.

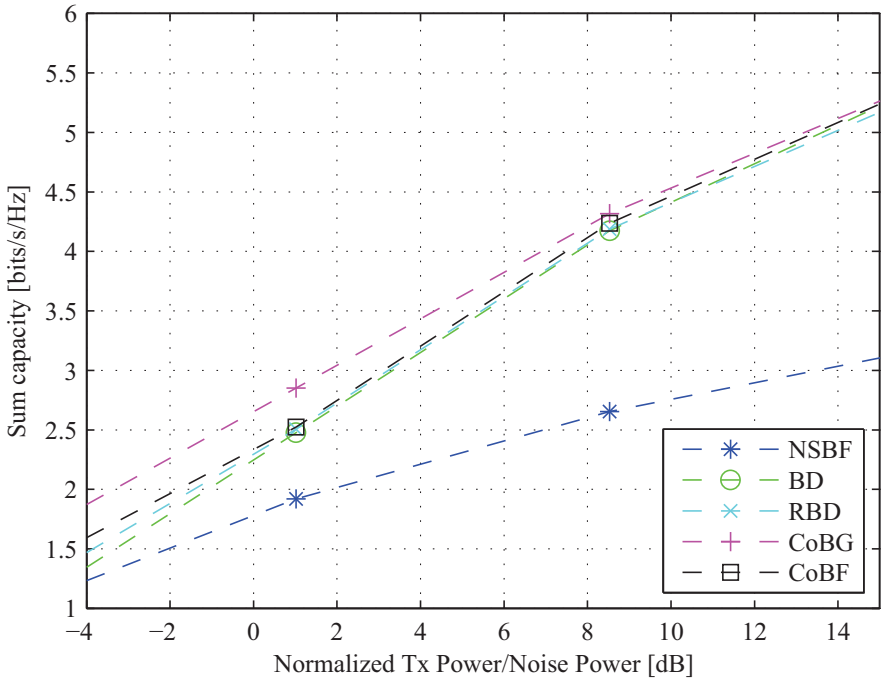

Figure 6.12: Measured capacity v.s. normalized Tx power to noise power ratio. NSBF: non-sharing case with MRT.

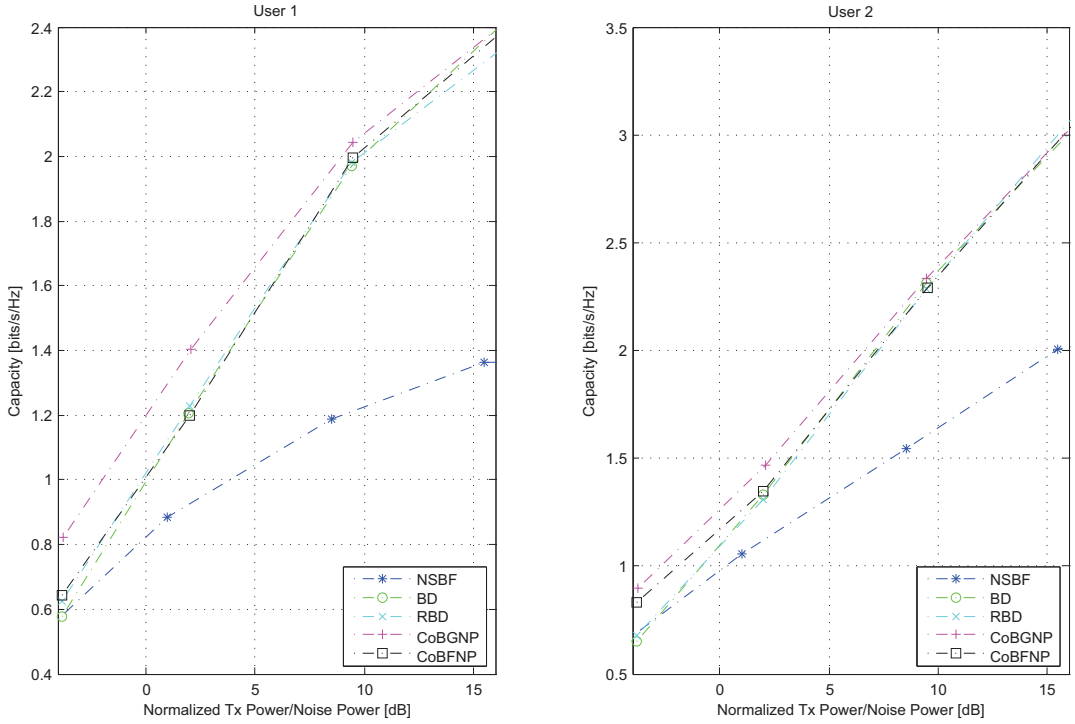

Figure 6.13: Measured per user capacity v.s. normalized Tx power to noise power ratio. NSBF: non-sharing case with MRT.

6.2 Scenario SC1-TB: Full Sharing

6.2.1 Scenario and Test Case Description

6.2.1.1 Scenario Description

This scenario is shown in Figure 6.14. This scenario consists of one BSs as well as multiple UTs of different operators. In Figure 6.14, an example with two operators is shown. The BS and each UT can be equipped with multiple antennas. These two operators share both the BS and the spectrum (completely). This means that in the downlink, the data streams from the different operators are transmitted in the same spectrum through the same Tx antennas of the BS. In the uplink, signals from both UTs will be received via the same Rx antennas of the BS. In this scenario, we mainly observe the downlink transmission, whose throughput is the most important measure. Full sharing poses challenge on the separation/multiplexing of both data steams and the dedicated delivery of the data. To achieve data stream multiplexing, either Tx- or Rx side signal processing techniques can be applied. On the Rx side, spatial multiplexing technique can be used to decode both transmitted data streams. However, in this case, both UTs see the data of the other operator. Due to privacy reasons, this is not desired. Thus, Tx side technique is more favorable. Tx side techniques also have the advantage that the signal processing complexity of the UTs can be relaxed. The most typical Tx side technique is advanced precoding techniques based on multiple Tx antennas. With appropriate precoding technique, the UTs can receive the dedicated data stream without complex decoding algorithm and without seeing the data stream of the other operator.

Within this scenario, we should show that with full sharing (aided by advanced precoding techniques developed in SAPHYRE), higher performance e.g. the total throughput, can be achieved than the case without full sharing (e.g. only BS sharing but no spectrum sharing). Since the precoding processing of both operators takes place in the same BS, perfect time synchronization of different operators can be achieved.

6.2.1.2 Test Case Description

For the test of this scenario on the demonstrator platform, the number of Tx antennas at the BS and number of Rx antenna at each UT are set to 2 and 1, respectively. OFDM is applied as the PHY technique. The total number of non-zero SubCarriers (SC) and NULL SCs can be flexible. The length of the Cyclic Prefix can also be flexible. Different channels can be used including Rayleigh channels, WINNER II channels [12] and measured LTE channels based on the LTE test field of FhG-HHI [11]. Different digital modulation waveforms can be applied e.g. BPSK, QPSK etc. We assume that no channel coding is applied. However, channel coding can

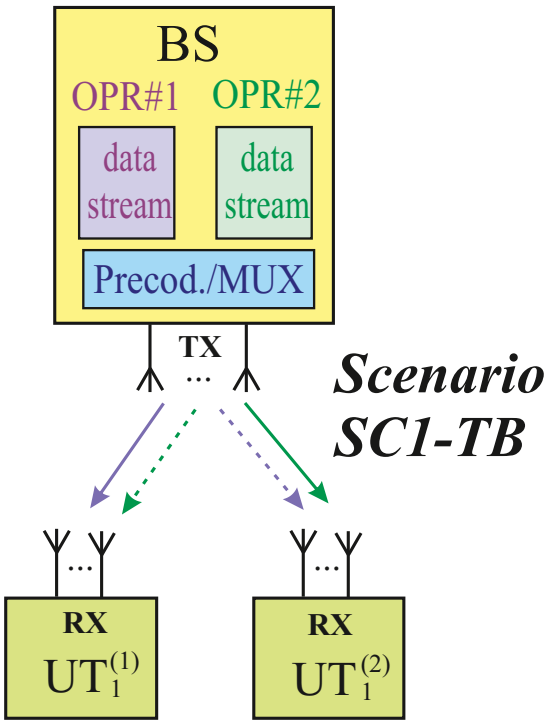

Figure 6.14: Scenario SC1-TB: Full sharing (spectrum and infrastructure sharing).

be included in the future. Finally, we assume that BS obtains all related channel information via feedback from the UTs.

We will make the following two comparisons:

- Infrastructure sharing without spectrum sharing (each operator uses a half of the available frequency band) and full sharing: To show the SAPHYRE gain. In order to have fair comparison, BF techniques are also applied in the non-sharing case within the own band of each operator;
- In the case of full sharing, different possible precoding techniques (algorithms) are compared: To identify suitable algorithms.

The used performance metrics are: sum rate (in bits/s/Hz), single user rate (in bits/s/Hz), throughput (in bits/s/Hz).

6.2.2 Enabling Algorithms

6.2.2.1 Precoding using Block-Diagonalization (BD) and Regularized Block-Diagonalization (RBD)

The BD [28] or RBD [29] has been designed to suppress the inter-user interference on the downlink of multi-user MIMO systems, which can be applied in the inter-operator full sharing scenario defined by SAPHYRE. Suppose there are K users shared the spectrum as well as the RAN. The base station (BS) is equipped with M_{T} antennas. The total receive antennas at user terminals (UTs) are denoted by M_{U} with each UT equipped with $M_{\mathrm{U},k}$ antennas. The detailed algorithms are summarized as follows.

The received signal at the user terminals (UTs) are written as

$$\begin{aligned}
\begin{bmatrix} y_1 \\ \vdots \\ y_K \end{bmatrix} &= \begin{bmatrix} \boldsymbol{g}_1^{\mathrm{H}} & & \\ & \ddots & \\ & & \boldsymbol{g}_K^{\mathrm{H}} \end{bmatrix} \begin{bmatrix} \boldsymbol{H}_1 \\ \vdots \\ \boldsymbol{H}_K \end{bmatrix} \begin{bmatrix} \boldsymbol{w}_1 & \dots & \boldsymbol{w}_K \end{bmatrix} \begin{bmatrix} s_1 \\ \vdots \\ s_K \end{bmatrix} \\
&\quad + \begin{bmatrix} \boldsymbol{g}_1^{\mathrm{H}} & & \\ & \ddots & \\ & & \boldsymbol{g}_K^{\mathrm{H}} \end{bmatrix} \begin{bmatrix} \boldsymbol{n}_1 \\ \vdots \\ \boldsymbol{n}_K \end{bmatrix} \\
&= \underbrace{\begin{bmatrix} \boldsymbol{g}_1^{\mathrm{H}}\boldsymbol{H}_1\boldsymbol{w}_1 & \dots & \boldsymbol{g}_1^{\mathrm{H}}\boldsymbol{H}_1\boldsymbol{w}_1 \\ \vdots & \ddots & \vdots \\ \boldsymbol{g}_K^{\mathrm{H}}\boldsymbol{H}_K\boldsymbol{w}_1 & \dots & \boldsymbol{g}_K^{\mathrm{H}}\boldsymbol{H}_K\boldsymbol{w}_K \end{bmatrix}}_{\boldsymbol{H}_e} \begin{bmatrix} s_1 \\ \vdots \\ s_K \end{bmatrix} + \begin{bmatrix} \boldsymbol{g}_1^{\mathrm{H}}\boldsymbol{n}_1 \\ \vdots \\ \boldsymbol{g}_K^{\mathrm{H}}\boldsymbol{n}_K \end{bmatrix}
\end{aligned}$$

where $\boldsymbol{w}_k$ is the precoding matrix at the BS. When block diagonalization (BD) is used, the off-diagonal elements in $\boldsymbol{H}_e$ are completely removed, which represent

the interference between users that belong to different operators. To do that, the null space of the combined interference channel for user k is first extracted, $k \in \{1, \cdots, K\}$. The singular value decomposition (SVD) is computed as $\tilde{\boldsymbol{H}}_k = \tilde{\boldsymbol{U}}_k \cdot \tilde{\boldsymbol{\Sigma}}_k \cdot \tilde{\boldsymbol{V}}_k^{\mathrm{H}} = \tilde{\boldsymbol{U}}_k \cdot \tilde{\boldsymbol{\Sigma}}_k \cdot \left[\begin{array}{cc} \tilde{\boldsymbol{V}}_k^{(1)} & \tilde{\boldsymbol{V}}_k^{(0)} \end{array} \right]^{\mathrm{H}}$. Denoting the rank of $\tilde{\boldsymbol{H}}_k$ by $\tilde{r}_k$, the signal space and the null space of $\tilde{\boldsymbol{H}}_k$ are obtained as $\tilde{\boldsymbol{V}}_k^{(1)} \in \mathbb{C}^{M_{\mathrm{T}} \times \tilde{r}_k}$ and $\tilde{\boldsymbol{V}}_k^{(0)} \in \mathbb{C}^{M_{\mathrm{T}} \times (M_{\mathrm{T}} - \tilde{r}_k)}$, respectively. After zero-forcing the inter-user interference, the SVD of the effective channel for user k is written as $\boldsymbol{H}_k \boldsymbol{V}_k^{(0)} = \boldsymbol{U}_k \cdot \boldsymbol{\Sigma}_k \cdot \boldsymbol{V}_k^{\mathrm{H}} = \boldsymbol{U}_k \cdot \boldsymbol{\Sigma}_k \left[\begin{array}{cc} \boldsymbol{V}_k^{(1)} & \boldsymbol{V}_k^{(0)} \end{array} \right]^{\mathrm{H}}$ for $k \in \{1, \cdots, K\}$, where the columns of $\boldsymbol{V}_k^{(1)} \in \mathbb{C}^{(M_{\mathrm{T}} - r_k) \times r_k}$ span the signal space of $\boldsymbol{H}_k$ projected into the null space of $\tilde{\boldsymbol{H}}_k$ with r_k denoting the rank of $\boldsymbol{H}_k \boldsymbol{V}_k^{(0)}$. In order to maximize the sum rate of the user k, the beamforming vector is obtained as $\boldsymbol{w}_k = \tilde{\boldsymbol{V}}_k^{(0)} \boldsymbol{v}_k^{(1)}$, where $\boldsymbol{v}_k^{(1)}$ is the first column of $\boldsymbol{V}_k^{(1)}$. The received filter $\boldsymbol{g}_k$ is derived as $\boldsymbol{g}_k = \boldsymbol{u}_k^{(1)}$ with $\boldsymbol{u}_k^{(1)}$ denoting the left dominant singular vector of $\boldsymbol{H}_k \boldsymbol{V}_k^{(0)}$.

Instead of zero-forcing the inter-user interference, regularized block diagonalization (RBD) is designed to maximize the system sum rate under the constraint that the Frobenius norm of the inter-user interference plus noise is minimized. The design of $\boldsymbol{w}_k = \beta \boldsymbol{W}_{k,a} \boldsymbol{w}_{k,b}$ is divided into two steps, where $\boldsymbol{W}_{k,a}$ is used to suppress the interference while $\boldsymbol{w}_{k,b}$ facilitates the rate optimization for user k. Additionally, we have a scalar β to fulfill the transmit power constraint at the BSs. Assuming that $||\boldsymbol{w}_{k,b}|| = 1$ and full-power transmission, we have $\beta^2 ||\boldsymbol{W}_{k,a} \boldsymbol{w}_{k,b}||^2 = \beta^2 ||\boldsymbol{W}_{k,a}||_F^2 = P_{\mathrm{T}}$. Therefore, we choose $\beta = \sqrt{P_{\mathrm{T}}} / ||\boldsymbol{W}_{k,a}||_F$. The matrix $\boldsymbol{W}_{k,a}$ is designed to minimize the Frobenius norm of the inter-user interference plus noise, i.e.,

$$\boldsymbol{W}_{k,a} = \min_{\boldsymbol{W}_{k,a}} E\{||\boldsymbol{H}_k \boldsymbol{W}_{k,a}||_F^2 + \frac{||\boldsymbol{n}||_2^2}{\beta^2}\},$$

where $\boldsymbol{n} = \left[\begin{array}{c} \boldsymbol{n}_1 \\ \vdots \\ \boldsymbol{n}_K \end{array} \right]$. After computing the SVD of the interference channel $\tilde{\boldsymbol{H}}_k = \tilde{\boldsymbol{U}}_k \cdot \tilde{\boldsymbol{\Sigma}}_k \cdot \tilde{\boldsymbol{V}}_k^{\mathrm{H}}$, we get $\boldsymbol{W}_{k,a} = \boldsymbol{M}_{k,a} \boldsymbol{D}_{k,a}$, where $\boldsymbol{M}_{k,a} = \tilde{\boldsymbol{V}}_k$ and $\boldsymbol{D}_{k,a} = (\tilde{\boldsymbol{\Sigma}}_k^{\mathrm{T}} \tilde{\boldsymbol{\Sigma}}_k + \frac{M_{\mathrm{U}} \sigma_n^2}{P_{\mathrm{T}}} \boldsymbol{I}_{M_{\mathrm{T}}})^{-\frac{1}{2}}$ is a diagonal power loading matrix. The matrix $\boldsymbol{D}_{k,a}$ is positive definite in order to get a nontrivial solution of $\boldsymbol{W}_{k,a}$. Similarly as BD, the effective channel after interference suppression is written as $\boldsymbol{H}_k \boldsymbol{W}_{k,a} = \boldsymbol{U}_k \cdot \boldsymbol{\Sigma}_k \cdot \boldsymbol{V}_k^{\mathrm{H}}$. The vector $\boldsymbol{w}_{k,b}$ is obtained as $\boldsymbol{w}_{k,b} = \boldsymbol{v}_k^{(1)}$ to enhance the sum rate for user k, where $\boldsymbol{v}_k^{(1)}$ is the right dominant singular vector of $\boldsymbol{H}_k \boldsymbol{W}_{k,a}$. The received filter $\boldsymbol{g}_k$ is derived as the left dominant singular vector of $\boldsymbol{H}_k \boldsymbol{W}_{k,a}$.

Both BD and RBD are closed-form solutions and no iterations are required, which makes it easy to implement. Furthermore, RBD improves the system sum rate performance at low SNRs compared to BD due to that it balances the inter-user interference with noise enhancement. At high SNRs, the sum rate performance obtained by BD and RBD converge. The drawback of BD algorithms is that the system is imposed on the antenna configuration constraint to assure the existence

of the null space, i.e., $M_T > M_U$. The RBD algorithm could be applied to any antenna configuration, but the sum rate performance degrade dramatically as SNR increases when $M_T \leq M_U$ due to that RBD turns out to extract the null space at high SNRs as BD does.

6.2.3 Practical Implementation Issues

The practical implementation problems in this scenario as well as the solutions are generally similar to those in the scenario SC2-TA, which have been described in Sec. 6.1.3.1 to Sec. 6.1.3.5.

6.2.4 Mapping on the HIL-Demonstrator Platform

For the test of the SC1-TB scenario, the BS and the UTs are mapped to the demonstrator platform both under channel emulator mode and the 60 GHz transmission mode. The latter one is illustrated in Fig. 6.15. As shown, two experimental devices are used. While the transmitter of one device acts the role of the BS, the receiver of the other device acts the roles of both UTs. Furthermore, similar to the mapping of scenario SC2-TA, one device acts as the master (w.r.t. trigger signal distribution etc.), while the other one acts as the slave. At the device acting BS, the outputs of the two modulators are connected to 60 GHz Tx antennas, which are directional antennas. At the device acting the UTs, the inputs of the demodulators are connected to the 60 GHz Rx antennas, which are omnidirectional antennas.

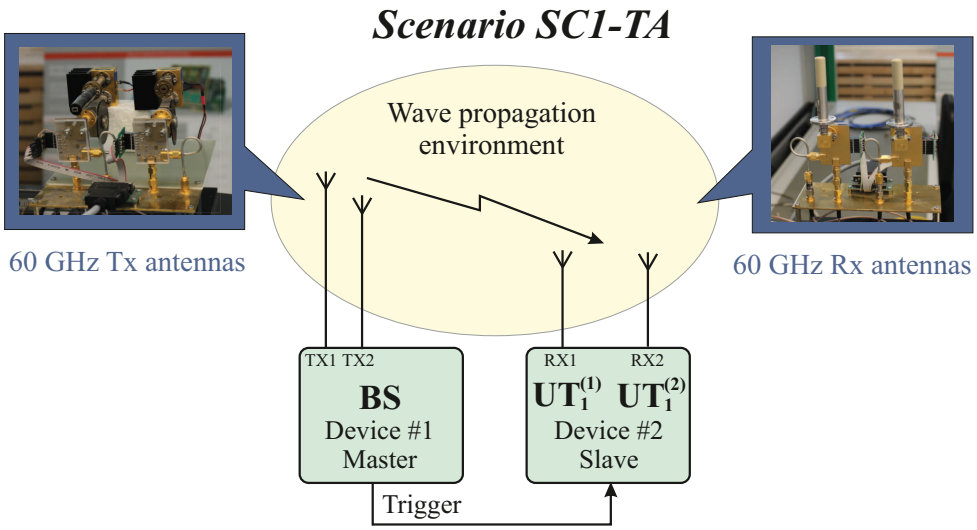

Figure 6.15: Mapping of scenario SC1-TB on the HIL platform with 60 GHz free space transmission mode

Fig. 6.16 shows the flowchart of the HIL test program. First, general parameter settings are carried out. Afterwards, the channel set up is carried out including the activation of the channel emulator mode or the 60 GHz transmission mode. In the case of channel emulator mode, the corresponding channel operations are the same as those in scenario SC2-TA. Afterwards, channel estimation (and noise power estimation) are carried out. Different SNR levels can be achieved by adjusting the variable gain amplifiers at the modulators. In the 60 GHz transmission mode, this can also be achieved by increasing the Tx-Rx distance. For each channel realization and each SNR level, signal transmissions with both non-sharing and sharing are carried out. In the sharing case, different precoding algorithms can be applied. During each transmission, some intermediate results e.g. the received signal constellation and the currently measured throughput can be shown. After all transmissions are finished, the results will be evaluated and saved.

6.2.5 Initial HIL-Test Results

In the HIL test with the 60 GHz transmission mode, OFDM signals with 256 subcarriers and CP length of 32 samples were transmitted. These numbers were chosen according to the propagation characteristics of the indoor 60 GHz channel and the bandwidth.

In the non-sharing case, each operator transmits in half of the available spectrum using EMBF (or so called MRT). This allows the comparison between the non-sharing and the sharing cases to be fare. In the sharing case, the proposed advanced precoding algorithm with BD is applied. The RBD and further algorithms will be included in the future. Fig. 6.17 shows the spectra of the transmitted signals in the non-sharing and sharing cases. Fig. 6.18 shows an example of the measured frequency response of the measured 60 GHz channels with Tx-Rx distance of about 2 meters.

Fig. 6.19 shows the measured received signal constellation (with QPSK) in the sharing case with BD precoding algorithm as well as in the non-sharing case with EMBF. Both the cases with and without additional Rx equalization are shown. As can be seen in the lower part of this figure, slight amplitude and phase distortion (probably due to channel variation or time synchronization error) of the constellations can be corrected by the additional Rx equalization. Interestingly, the noise and interference level of constellations in the sharing cases and the non-sharing case are almost the same. Note that in this result, the noise and interference levels of both the sharing and non-sharing cases are similar (unlike the cases in Fig. 6.10). The reason may be the favorable instant channels for the separation of the two data streams. More interference is expected in the sharing case if the channels to different UTs become more correlated.

Fig. 6.20 shows the instantaneous measured sum throughput of the different cases. As shown, the sharing cases have much higher throughput than the non-sharing

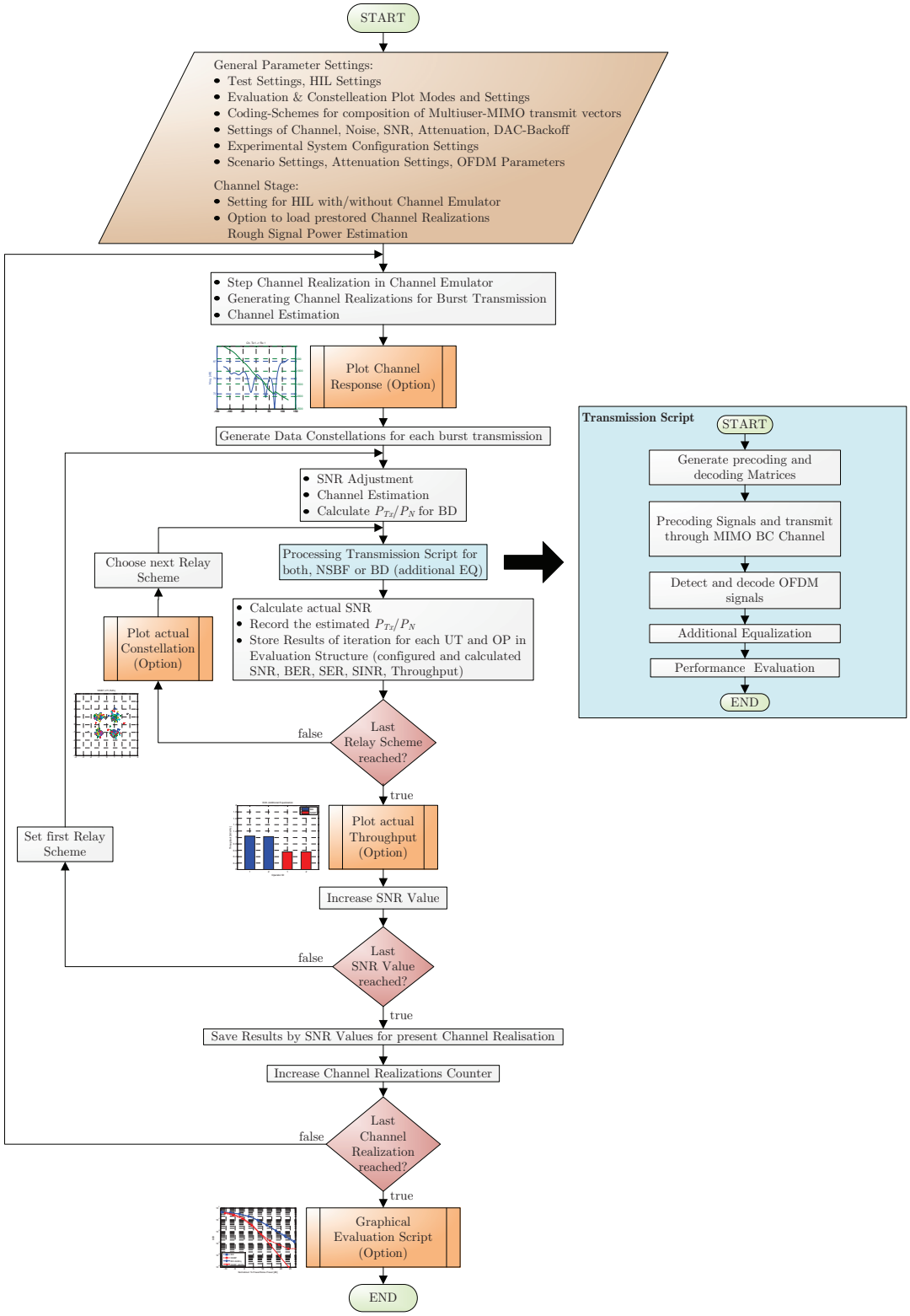

Figure 6.16: Flowchart of the software implementation of the full sharing scenario.

case. Moreover, in the non-sharing case, the additional equalization has improved the throughput. Note that the benefit of additional Rx equalization is not only in the non-sharing case. If amplitude and phase distortion also exist in the sharing case, the additional Rx equalization can also provide improvement.

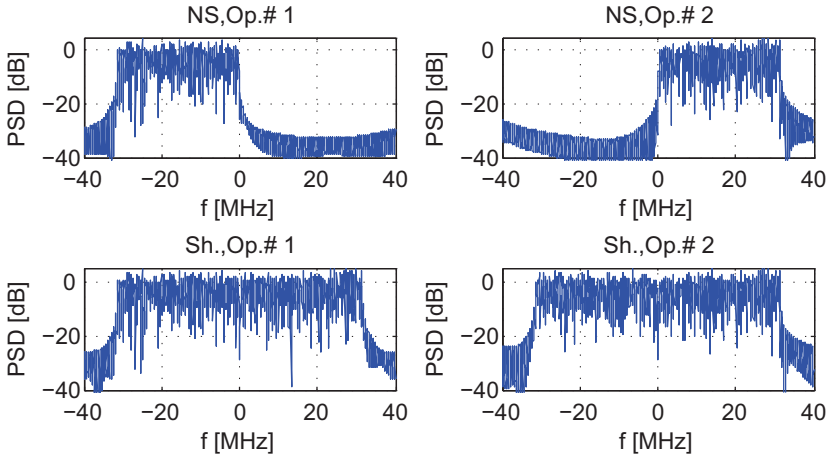

Figure 6.17: Spectra of the transmitted signals in the non-sharing and sharing cases.

6.2.6 Future Works

In the future, more algorithms should be integrated including RBD and the sum rate maximization based algorithm. Moreover, a systematical HIL test will be carried out with the channel emulator mode applying the measured LTE channels. The different precoding algorithms will be compared in order to identify the most suitable one.

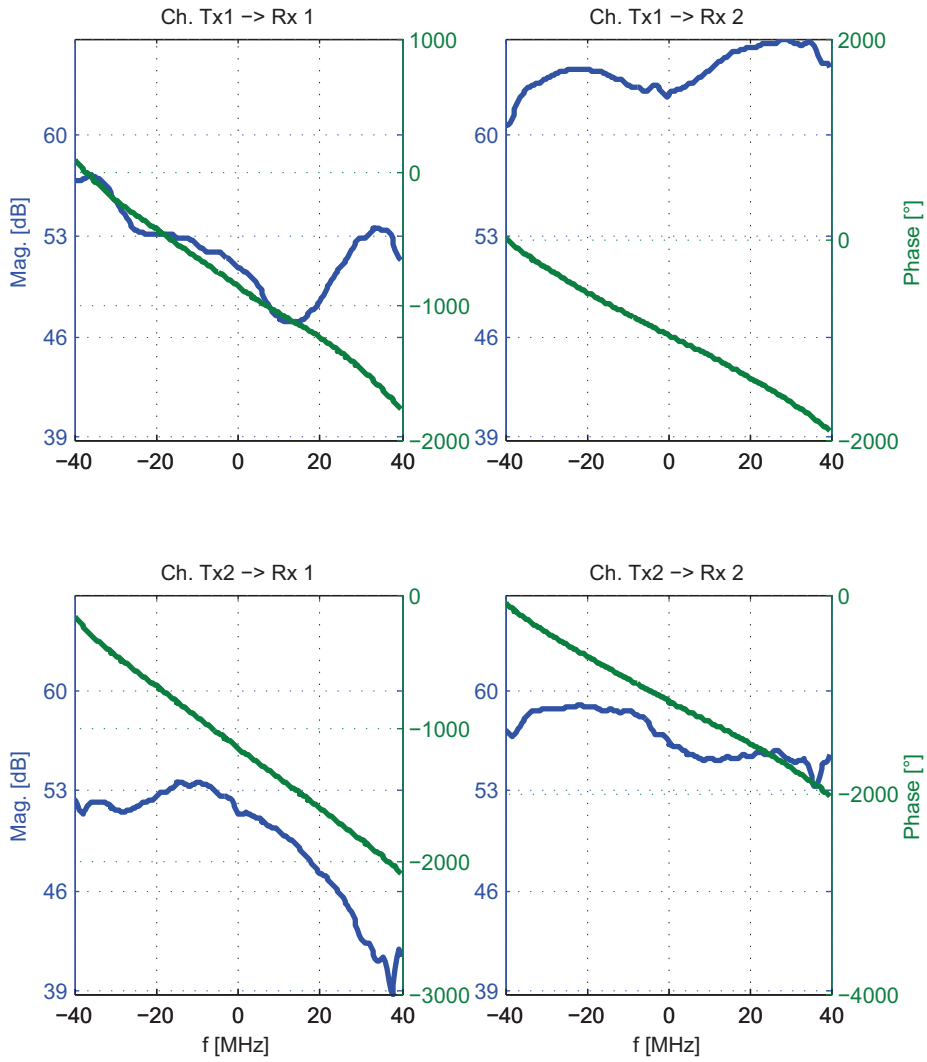

Figure 6.18: Frequency response of the measured 60 GHz channels.

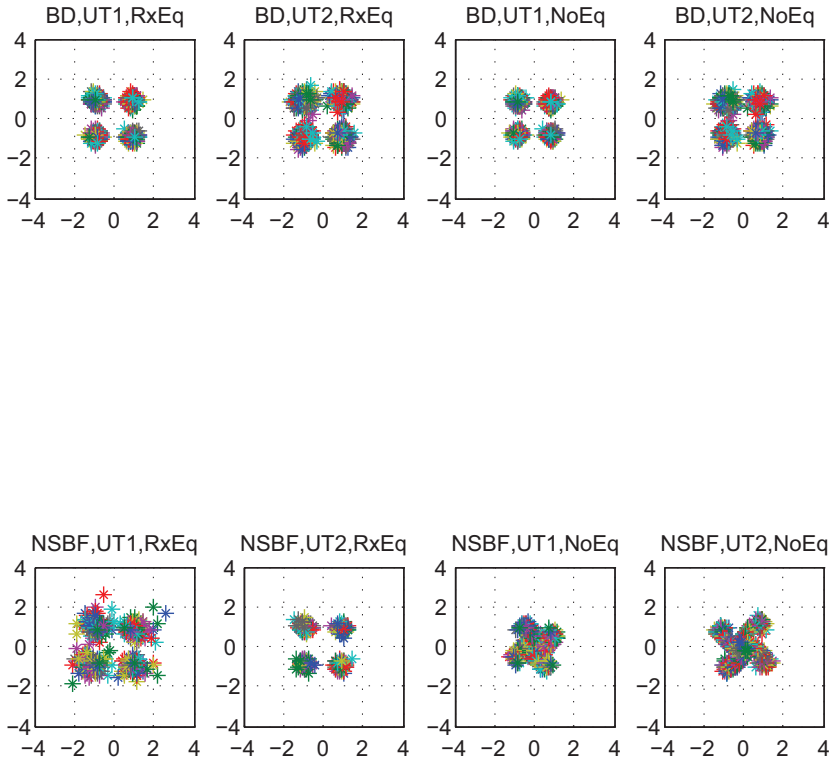

Figure 6.19: Measured received signal constellation in the sharing and non-sharing cases. Both the cases with and without additional Rx equalization are shown.

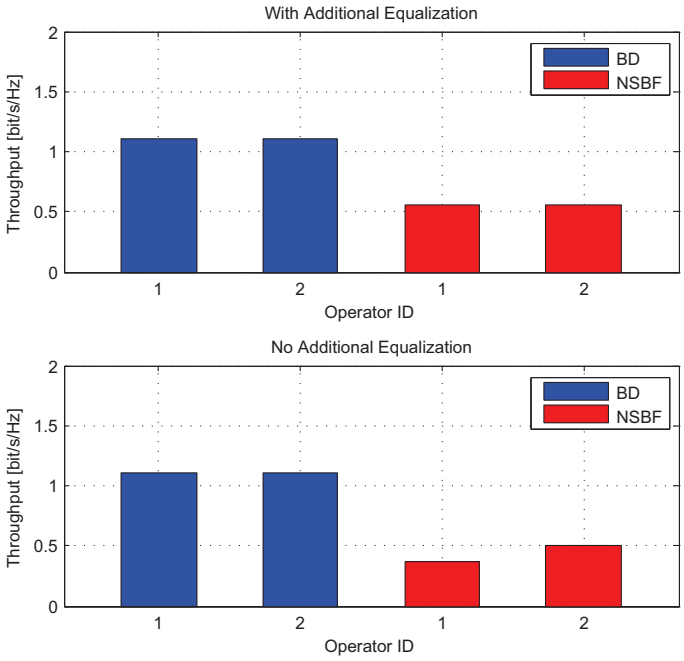

Figure 6.20: Measured received signal constellation with different BF algorithms as well as in the non-sharing case. Both the cases with and without additional Rx equalization are shown.

6.3 Scenario SC1-TC-I: Relay Sharing in "Butterfly" Network

6.3.1 Scenario and Test Case Description

6.3.1.1 Scenario Description

As shown in Figure 6.22, this scenario consists of a "butterfly" network topology, where two independent data sources, SA and SB, of different operators should transmit data to the destinations DA and DB, respectively, via two-phase relaying transmission. Both relay station and spectrum are shared between operators. In the Multiple Access (MAC[8]) phase, SA and SB transmit data to the relay and to the destinations DB and DA, respectively. Note that there is no direct link between a source and its dedicated destination. The received data of DA and DB in the MAC phase are called Complementary-Side-Information (CSI, [31]). In the BroadCast (BC) phase, the relay transmits data to both destinations. The destinations decode the dedicated data based on the data from the relay and the CSI. Since both relay and spectrum are shared, the data streams of SA and SB will be superimposed at the relay and cause interference to each other. To suppress such interference and achieve maximum capacity, sophisticated relaying strategy should be applied.

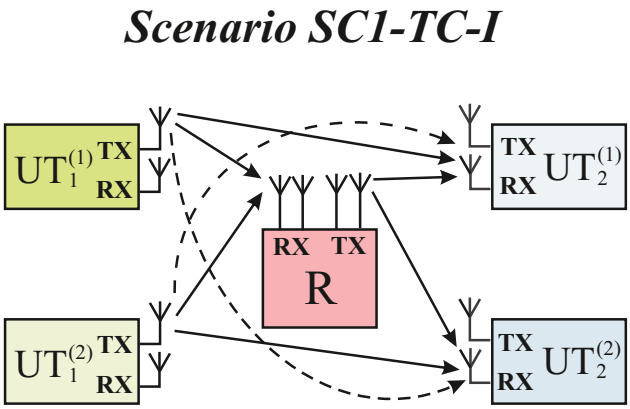

Figure 6.21: Scenario SC1-TC-I.

[8]Only within Ch. 6.3 and Ch. 6.4, the abbreviation "MAC" is used to indicate "Multiple Access".

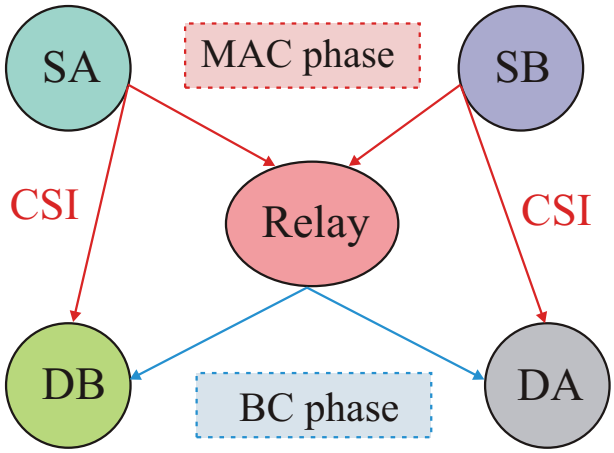

Figure 6.22: Abstracted model of Scenario SC1-TC-I.

6.3.1.2 Test Case Description

As PHY-layer technique, OFDM with BPSK modulation and LDPC coding of code rate $\frac{1}{2}$ is applied. The OFDM parameters are similar to those in scenario SC2-TA (Ch. 6.1). Rayleigh channels, WINNER II channels [12] or measured LTE-channels can be used. Moreover, single antenna transmission and global time synchronization are assumed.

As reference, the case without spectrum sharing is also tested, where the two sources use orthogonal frequency bands. Thus, without spectrum sharing, no interference is present between operators and the relay applies normal Decode-and-Forward (DF) strategy. Orthogonal frequency bands are used, the available frequency band for each operator is only the half of those in the spectrum sharing cases.

Two performance criteria are applied. The first one is the sum rate of the whole network in bits/s/Hz, which is mainly evaluated for coded transmissions. For the calculation of the sum rate, the CP and NULL-subcarrier overhead of the OFDM system as well as the transmission overhead of the two-phase-relaying are considered. The second one is the sum capacity in bits/symbol, which is evaluated both for uncoded and coded transmissions. Both criteria will be evaluated for different Rx SNR values as well as different SNR values in the CSI links. For simplicity, we assume that the Rx SNR (at the relay) in the MAC-phase is always equal to the Rx SNR in the BC-phase (at the destinations). Moreover, all CSI links should have the same SNR value.

6.3.2 Enabling Algorithms

Two relaying strategies are applied for interference suppression and capacity maximization: Hierarchical Decode and Forward (HDF, [31]) and Amplify-and-Forward with Successive Interference Cancellation (AF-SIC, [25]). The HDF strategy is developed within SAPHYRE project, while AF-SIC is a conventional strategy. For the OFDM system under investigation, both techniques are applied subcarrier-wise. These two strategies are briefly described as follows, assuming frequency-flat channels (which is the equivalent case within each OFDM subcarrier):

6.3.2.1 Hierarchical Decode and Forward (HDF)

We assume the coder $\mathcal{C}$ to be a LDPC coder and $\mathcal{M}$ the BPSK mapper. Also $\mathcal{M}^{-1}$ to be the soft output BPSK demodulator based on the minimal Euclidean distance and $\mathcal{C}^{-1}$ to be the LDPC decoder. There are assumed i.i.d. data vectors $\boldsymbol{d}_A$ and $\boldsymbol{d}_B$ inputing the LDPC coders $\mathcal{C}$. The output codewords $\boldsymbol{c}_A = C(\boldsymbol{d}_A)$ and $\boldsymbol{c}_B = C(\boldsymbol{d}_B)$ then input the BPSK signal space mapper $\mathcal{M}$ to form the output signal space vectors $\boldsymbol{s}_A = \mathcal{M}(\boldsymbol{c}_A)$ and $\boldsymbol{s}_B = \mathcal{M}(\boldsymbol{c}_B)$. The signal inputing the relay R is $\boldsymbol{x}_R = \boldsymbol{s}_A h_{AR} + \boldsymbol{s}_B h_{BR} + \boldsymbol{w}_{MAC}$, while the signal inputing the destination D_A is $\boldsymbol{y}_A^{MAC} = \boldsymbol{s}_B + \boldsymbol{w}_{BA}$. Moreover, the signal inputing the destination D_B is $\boldsymbol{y}_B^{MAC} = \boldsymbol{s}_A + \boldsymbol{w}_{AB}$. Within the relay, the minimal Euclidean metric

$$\mu_{AB}^k = \min_{i,j:k=\mathcal{X}(i,j)} |x_R - s_A^i h_{AR} - s_B^j h_{BR}|^2$$

is evaluated in the relay (outer code caring about the exclusivity). Then the hierarchical data are decoded by $\hat{\boldsymbol{d}}_{AB} = \mathcal{C}^{-1}(\boldsymbol{\mu}_{AB})$ (inner code caring about the coding gain). The signal space vector inputing the BC-phase is given by $\boldsymbol{s}_R = \mathcal{M}(\mathcal{C}(\hat{\boldsymbol{d}}_{AB}))$. In the BC phase, the signal inputing the destination D_A is $\mathbf{y}_A^{BC} = \boldsymbol{s_R} + \boldsymbol{w}_{BC}$, whereas the signal inputing the destination D_B is $\mathbf{y}_B^{BC} = \boldsymbol{s_R} + \boldsymbol{w_{BC}}$. At the destination, the following C-SI's are used: $\boldsymbol{d}_A^{C-SI} = \mathcal{C}^{-1}(\mathcal{M}^{-1}(\boldsymbol{y}_B^{MAC}))$ and $\boldsymbol{d}_B^{C-SI} = \mathcal{C}^{-1}(\mathcal{M}^{-1}(\boldsymbol{y}_A^{MAC}))$. First, the relay-decoded hierarchical data $\hat{\hat{\boldsymbol{d}}}_{AB} = \mathcal{C}^{-1}(\mathcal{M}^{-1}(\mathbf{y}_A^{BC})$ is decoded. Finally, by exploiting the C-SI $\boldsymbol{d}_B^{C-SI}$, the data vector is decoded as: $\hat{\boldsymbol{d}}_A = \hat{\hat{\boldsymbol{d}}}_{AB} \oplus \boldsymbol{d}_B^{C-SI}$, where $\oplus$ denotes bit-wise XOR operation.

6.3.2.2 Amplify-and-Forward with Successive Interference Cancellation (AF-SIC)

The main signal transmission process of with AF-SIC is generally the same as with HDF. The main differences are the relay processing and the destination processing. With AF-SIC strategy, the relay transmits $\boldsymbol{s}_R = \boldsymbol{x}_R \beta$, where $\beta = 1/\sqrt{h_{AR}^2 + h_{BR}^2 + N_0}$ (see [25]). At the destination A, the signal is reconstructed from the C-SI as follows: $\boldsymbol{s}_A^{C-SI} = (\boldsymbol{y}_A^{BC} - h_{BR}\mathcal{M}(\mathcal{C}(\boldsymbol{d}_B^{C-SI})))/h_{AR}$ and the data $\hat{\boldsymbol{d}}_A = \mathcal{C}^{-1}(\mathcal{M}^{-1}(\boldsymbol{s}_A^{C-SI})$. The

reconstruction of $\hat{\boldsymbol{d}}_B$ follows a similar way. Note that the two way relaying in [25] can be regarded as the special case that SA=DB and SB=DA, which implies perfect CSI. Thus, the 2-step scheme in [25] can be easily extended to "butterfly" network.

6.3.3 Practical Implementation Issues

In this scenario, no BF- or precoding techniques are applied. Therefore, some the practical implementation problems mentioned in Sec. 6.1.3 are not relevant. First, since the channel estimation and the corresponding signal equalization are carried out within the same signal frame, these two procedures are consistent. Moreover, time synchronization error that is within the tolerable range of CP just changes the effective channel, which will be corrected by the channel equalization. Moreover, rate estimation is not necessary. However, the signal amplitude scaling for DACs and the rescaling of the channel coefficients are necessary. The effect of colored noise should also be considered.

Furthermore, the assumption of no direct link between each source and its dedicated sink may not be realistic. In the reality, there could still be weak links between each source and its dedicated sink, which is not sufficient for data detection but can disturb the reception of the CSI. Thus, slightly corrupted CSI links must be taken into account. In our HIL test, we have tested the cases with CSI of different SNR levels, which can more or less equivalent model the disturbance from the direct links. It will be shown that the proposed algorithms can work well even in the case of bad CSI quality.

Note that a very favorable character of this scenario is that no channel coefficient feedback is required.

6.3.4 Mapping on the HIL-Demonstrator Platform

For the initial test of this scenario, the mapping was done for the RF cable network mode assisted with multi-stage mapping technique. For simplicity, only one physical transmitter and one physical receiver were used. With multi-stage mapping, the desired scenario with three transmitters (SA, SB, relay) and three receivers (DA, DB, relay) can be mapped. In the future, this scenario can be mapped with the channel emulator mode. With this mode, the same numbers of transmitters and receivers as in the actual scenario will be applied.

Fig. 6.23 shows the flowchart of the HIL test program. First, general parameter settings are carried out. Afterwards, the channel set up is carried out including the selection of the channel mode and the loading of the channel files. Afterwards, channel realization control and channel estimation are carried out. With each channel realization, different SNR levels are applied by adding artificial noise or by adjusting the variable gain amplifiers at the modulators. For each channel realization and

each SNR level, signal transmissions in the H-MAC and the H-BC phases with both non-spectrum sharing and spectrum sharing are carried out one after another. In the sharing case, different relay algorithms are applied. During each transmission, some intermediate results e.g. the histogram of the soft bits at the input- and output of the LDPC decoder and the currently measured throughput can be shown. After all transmissions are finished, the results will be evaluated and saved.

6.3.5 Initial HIL-Test Results

In the HIL test, OFDM signals with 256 subcarriers and CP length of 32 samples were transmitted. In the non-sharing case, each operator transmits in half of the available spectrum using a normal DF relaying scheme.

Figure 6.24, Figure 6.25 and Figure 6.26 show the coded sum rates of the non-sharing case and the AF-SIC- and HDF strategies, respectively. As shown, without sharing, the sum rate is relatively low i.e. with a maximum of 0.17 bits/s/Hz. In both sharing cases, the maximum sum rate has achieved 0.35 bits/s/Hz. Note that the maximum sum rate is limited by the BPSK modulation. Thus, after the SNR has achieved a certain value, the sum rate remains constant in spite of further SNR increase.

Figure 6.27 and Figure 6.28 show the coded sum rate difference between the AF-SIC- as well as the HDF and the non-sharing case, respectively. As shown, the AF-SIC only has higher coded sum rate than the non-sharing case in about half of the investigated SNR region. In contrast, the HDF has higher coded sum rate than the non-sharing case in about $\frac{2}{3}$ of the total SNR region. These results prove that with spectrum sharing as well as applying the suitable sharing techniques, higher sum rate can be achieved. In other words, the SAPHYRE-gain is shown by these results.

Now, we compare the performance of both relaying strategies. Figure 6.29 shows the sum capacity in bits/symbol of the AF-SIC and HDF with uncoded and coded transmission in different SNR regions. As shown, with uncoded transmission, the areas of the full sum capacity SNR regions of HDF and AF-SIC are similar. However, with coded transmission, full sum capacity SNR region of HDF is much larger than that of AF-SIC.

Figure 6.30 and Figure 6.31 show the sum capacity difference between both techniques and the non-sharing case. As shown, in the uncoded case, HDF only has advantage against AF-SIC for a relatively small range of SNR and relatively large SNR_{CSI}. In contrast, with coded transmission, HDF has better performance than AF-SIC in the major part of the investigated SNR region (which is realistic). Only with very low SNR of CSI and relatively high SNR of the MAC- and BC links, AF-SIC has considerable advantage over HDF. Thus, we can conclude that in the coded case, the HDF is more robust than AF-SIC for the observed resource sharing

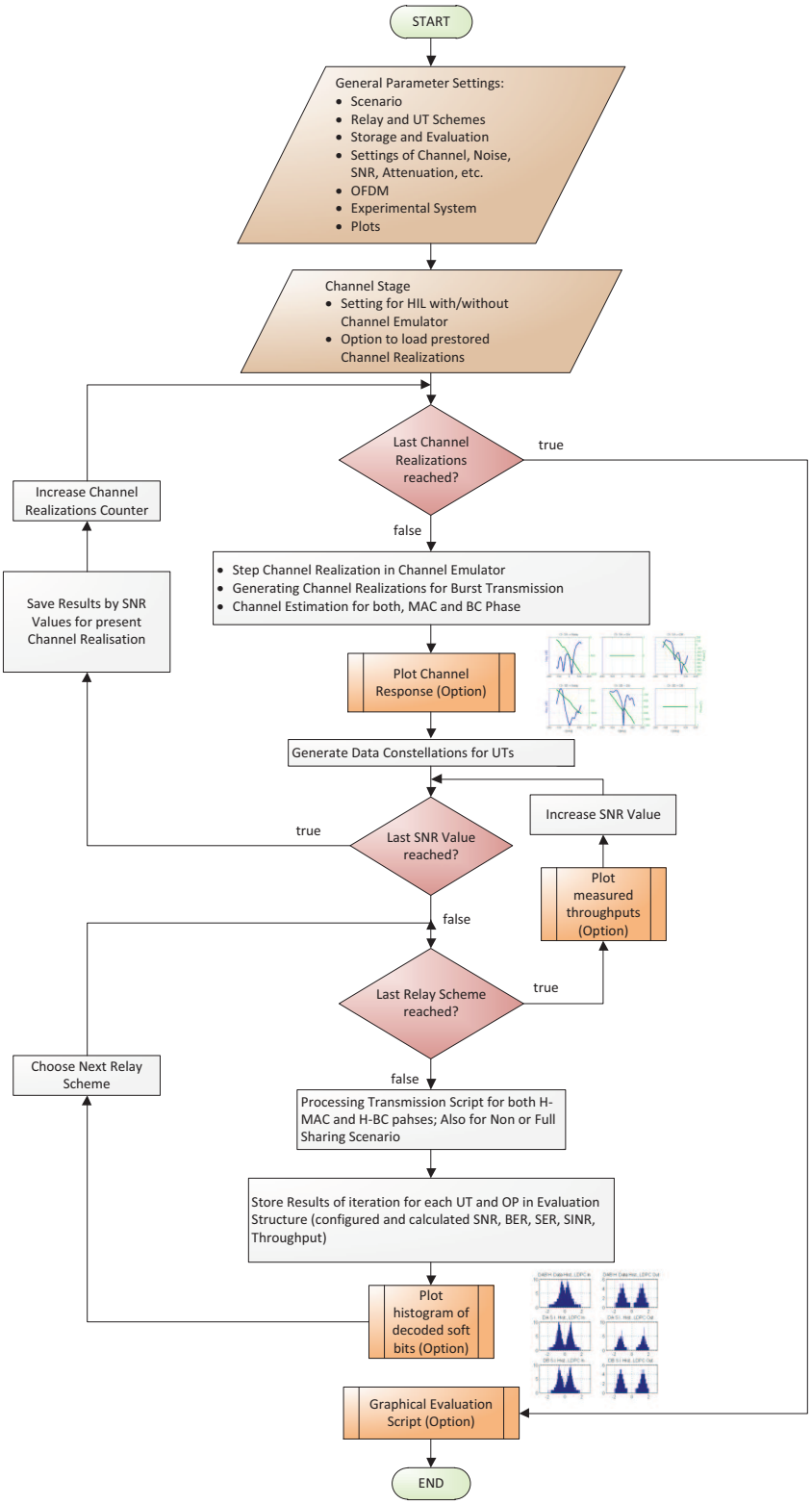

Figure 6.23: Flowchart of the software implementation of the relay sharing scenario with "butterfly" network.

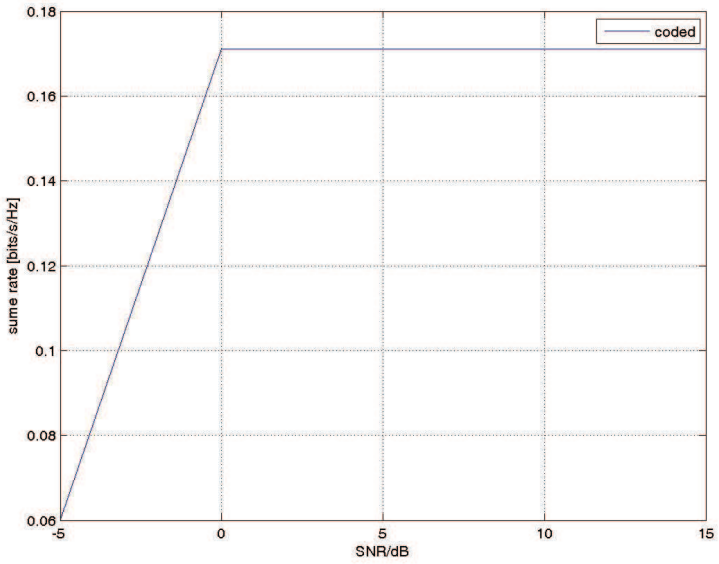

Figure 6.24: Reference scenario: coded sum rate of non-sharing case.

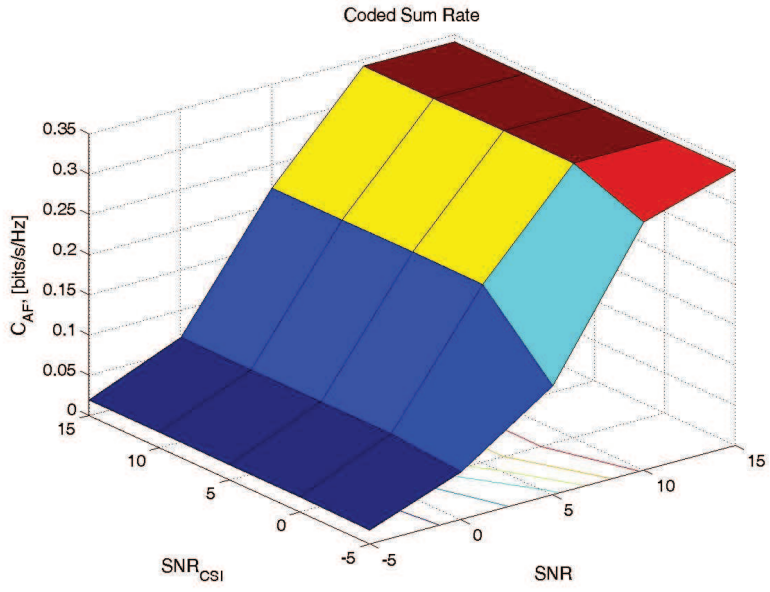

Figure 6.25: Scenario S1-TC-I: coded sum rate of AF-SIC strategy with spectrum sharing.

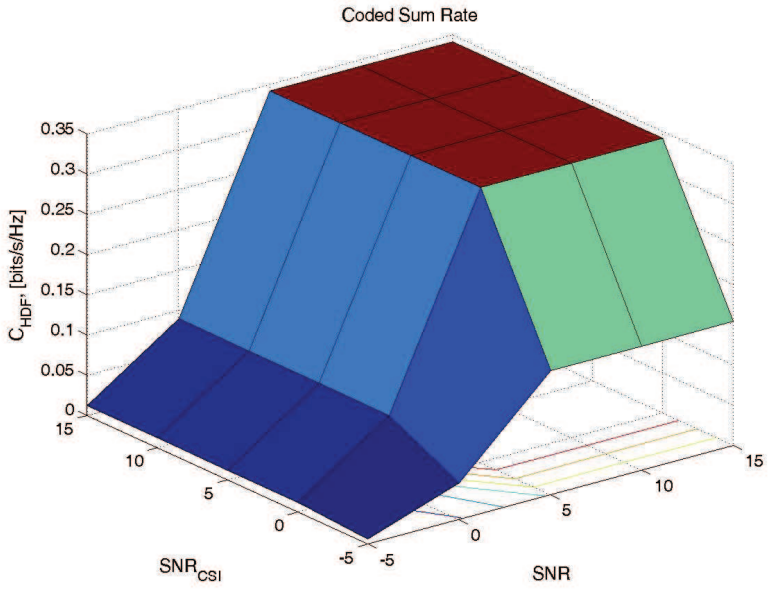

Figure 6.26: Scenario S1-TC-I: coded sum rate of HDF strategy with spectrum sharing.

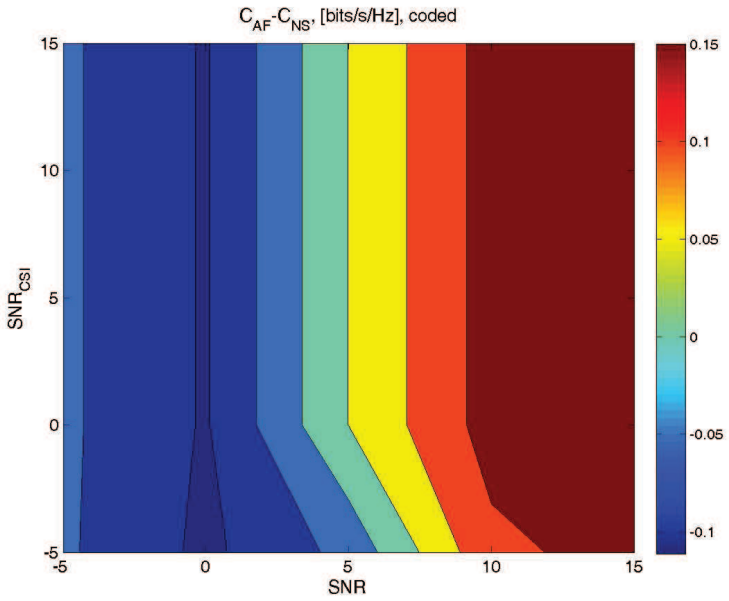

Figure 6.27: Scenario S1-TC-I: coded sum rate difference between AF-SIC and the non-sharing case.

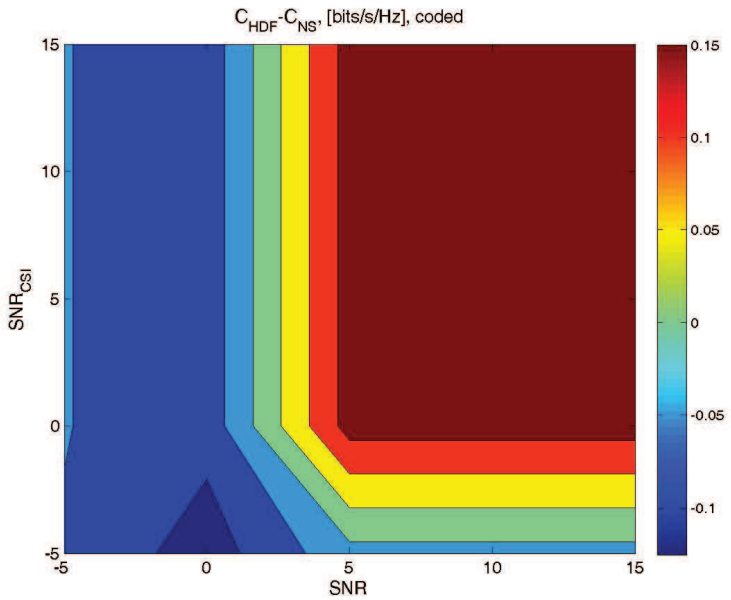

Figure 6.28: Scenario S1-TC-I: coded sum rate difference between HDF and the non-sharing case.

scenario.

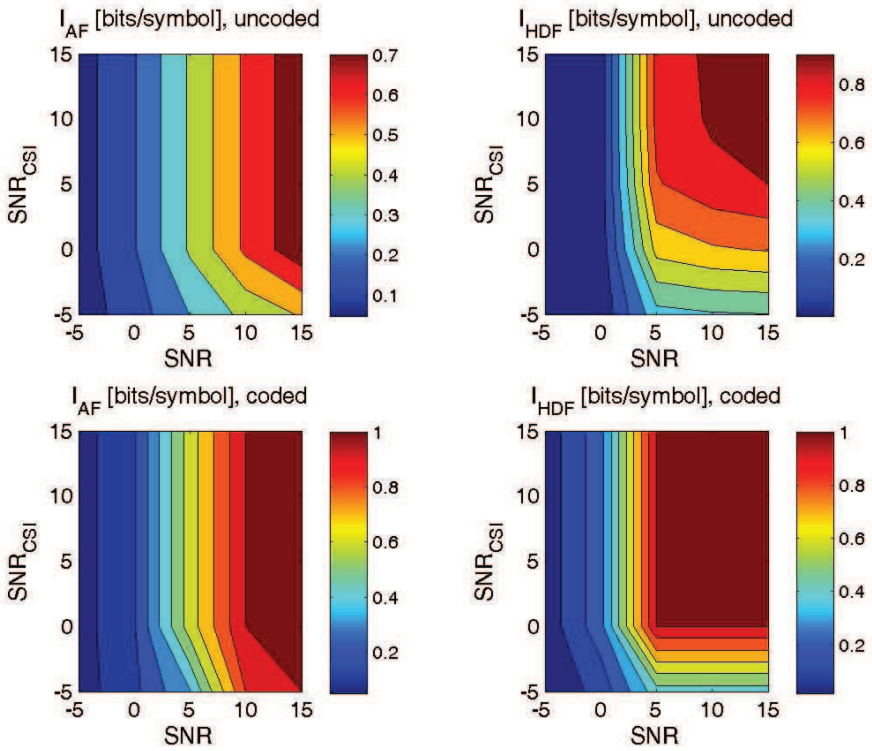

Figure 6.29: Scenario SC1-TC-I: capacity of HDF and AF-SIC with uncoded and coded transmission in different SNR regions.

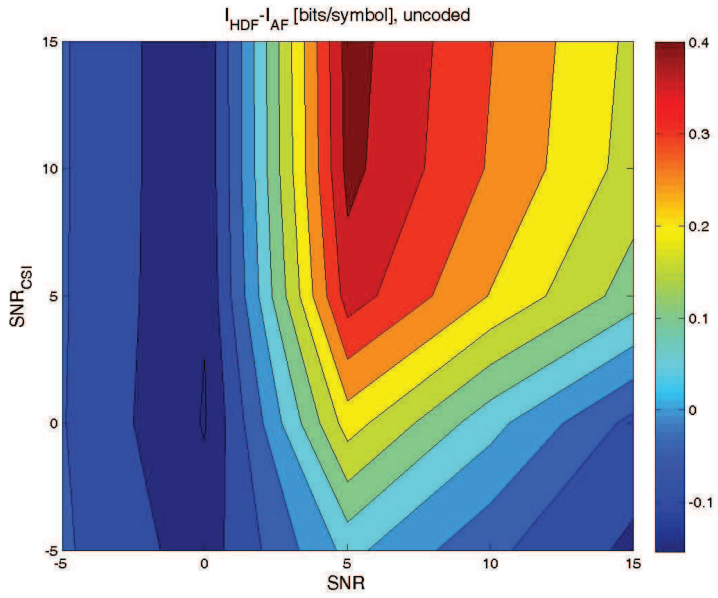

Figure 6.30: Scenario SC1-TC-I: capacity difference of HDF and AF-SIC with uncoded transmission in different SNR regions.

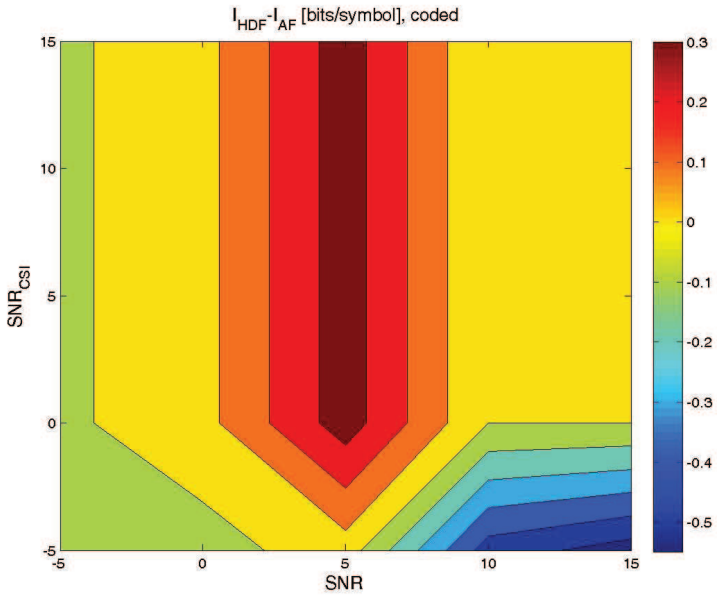

Figure 6.31: Scenario SC1-TC-I: capacity difference of HDF and AF-SIC in coded transmission in different SNR regions.

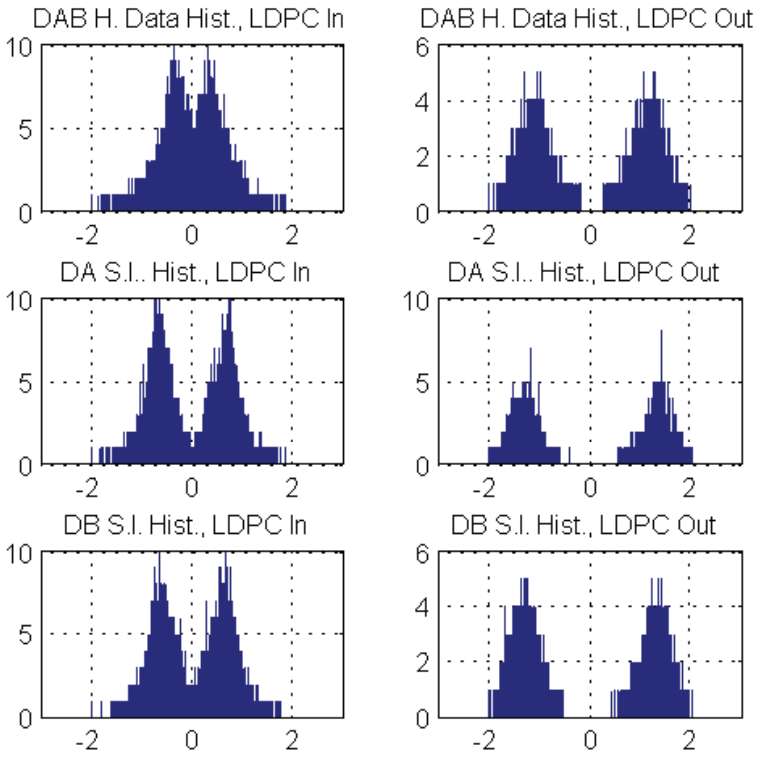

Figure 6.32: Scenario SC1-TC-I: Histogram of the soft bits before and after LDPC decoding in the HMAC phase, including the hierarchical bits of the HDF scheme and the CSI bits.

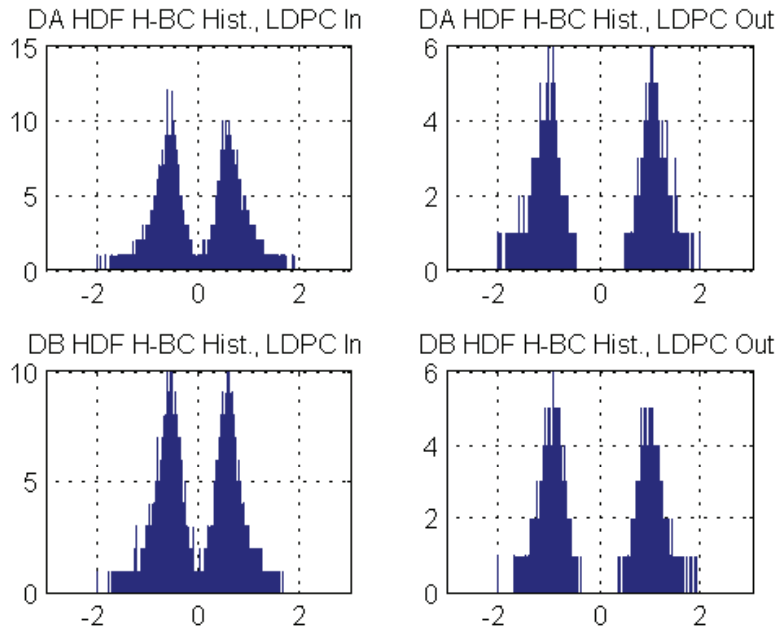

Figure 6.33: Scenario SC1-TC-I: Histogram of the soft bits of the HDF scheme before and after LDPC decoding in the HBC phase.

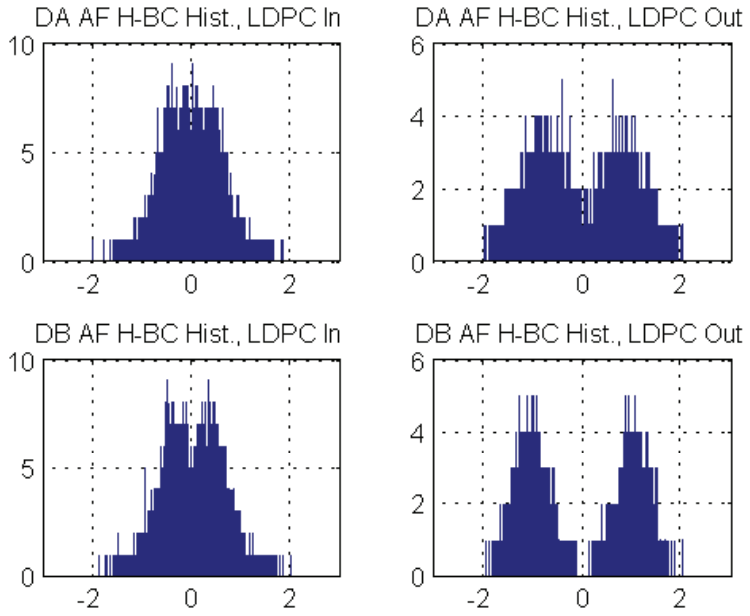

Figure 6.34: Scenario SC1-TC-I: Histogram of the soft bits of the AF scheme before and after LDPC decoding in the HBC phase.

6.3.6 Future Works

In the future, the mapping to demonstrator platform with the channel emulator mode will be implemented and the measured LTE channels will be used for test. New algorithms may be integrated.

6.4 Scenario SC1-TC-II: Relay Sharing in Two-Way-Relaying Network

6.4.1 Scenario and Test Case Description

6.4.1.1 Scenario Description

Figure 6.35 describes a Two-Way-Relaying (TWR) scenario with both relay and spectrum sharing by two different operators. In this scenario, multiple communication partners (owned by different operators) use one relay terminal (possibly owned by another operator/virtual operator) to bidirectionally exchange information using the same spectrum. All terminals as well as the relay have multiple antennas and operate in half-duplex mode. The TWR consists of two phase: the MAC-phase and the BC-phase. In the MAC-phase, all UTs transmit data to the relay. In the BC-phase, the relay broadcast data to all UTs. This broadcast data was calculated by the relay according to its received data in the MAC-phase. The relay station must take into account the fact that multiple operators are active and manage the interference they cause to each other according to their voluntary agreements.

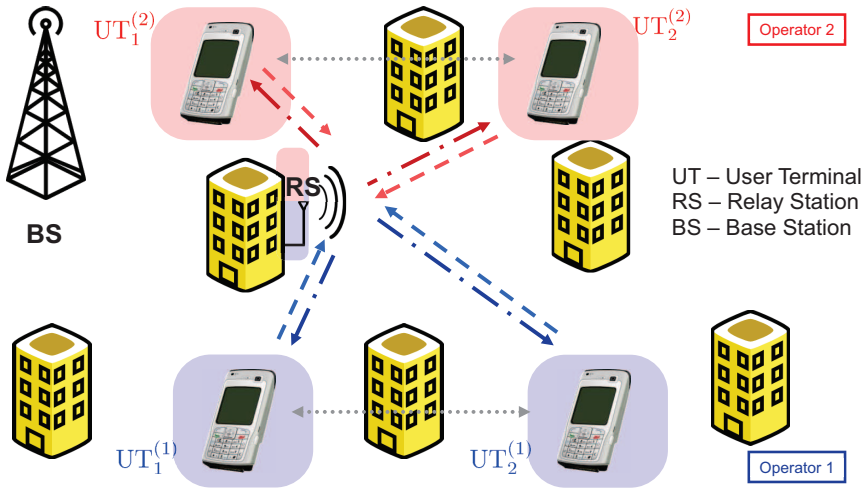

Figure 6.35: Scenario SC1-TC-II: Two Way Relaying (TWR) with multiple links of different operators sharing both the relay and the spectrum.

6.4.1.2 Test Case Description

For the test of this scenario on the demonstrator platform, we set the numbers of both Tx/Rx antennas at the relay to be 4. All UT have only single Tx and Rx

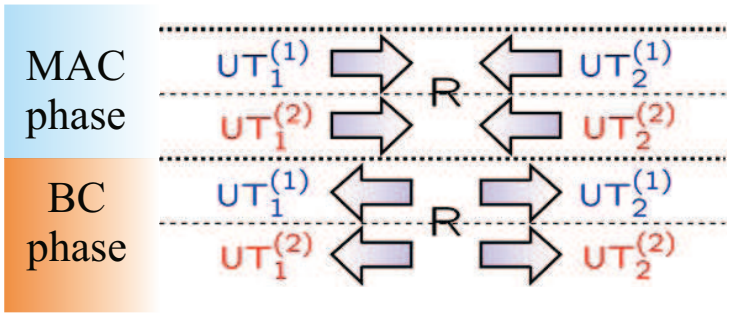

Figure 6.36: Scenario SC1-TC-II: Illustration of the MAC- and BC phases of the TWR procedure.

antennas, respectively. OFDM is applied as the PHY technique. The total number of non-zero SubCarriers (SC) and NULL SCs can be flexible. The length of the Cyclic Prefix can also be flexible. Different channels can be used including Rayleigh channels, WINNER II channels [12] and measured LTE channels. Different digital modulation waveforms can be applied e.g. BPSK, QPSK etc. We assume that no channel coding is applied.

We will make the following two comparisons:

- Spectrum sharing and non-spectrum sharing. In the non-spectrum sharing case, each operator uses a half of the available frequency band;
- In the case of spectrum sharing, different possible relaying techniques (algorithms) are compared: To identify suitable algorithms.

The used performance metrics are: sum rate (in bits/s/Hz), single user (operator) rate (in bits/s/Hz) and throughput (in bits/s/Hz).

6.4.2 Enabling Algorithms

6.4.2.1 System Model

The system model is derived from the scenario depicted in Fig. 6.35 and Fig. 6.36. We assume that pairs of users belonging to the same operator would like to communicate with each other. Therefore, the relay station must take into account the fact that multiple operators are active and manage the interference they cause to each other according to their voluntary agreements. The relay is equipped with M_{R} antennas and uses amplify and forward two-way relaying. Moreover, the k-th terminal belonging to the ℓ-th operator has $M_k^{(\ell)}$ antennas.

The traditional solution to avoid inter-operator interference is to assign orthogonal resources to the two groups, e.g., different frequencies (FDMA) or different time slots (TDMA). Consequently, for each group, any single-operator two-way relaying

techniques can be applied, e.g., the algebraic norm-maximizing transmit strategy (ANOMAX) [26]. This corresponds to the case of exclusive frequency bands and physically separated infrastructure. However, by using this scheme the individual sum data rate of each operator decreases by a factor of two since the time slots have to be shared. Therefore, in order to investigate the potential gain from voluntary infrastructure sharing, we propose an SDMA-based approach that allows both operators to serve their users via a physically shared relay by taking advantage of multiple antennas at the relay. This implies that the operators agree to voluntarily share their infrastructure and their spectrum in a coordinated manner. As we demonstrate, this form of cooperation not only reduces the operators' expenditure but additionally provides them with an improvement in the overall sum rate, since the resources are used more efficiently. These benefits provide the motivation for the operators to share their spectrum as well as their infrastructure. Our procedure consists of two steps. In the first step, the system is converted into two parallel independent sub-systems. Then, in the second step, arbitrary transmission techniques for single-operator two-way relaying can be applied. Note that this two-step approach is used here only for simplicity since it is in general suboptimal.

As in the basic two-way relaying scenario, where two users exchange data with the help of one relay, all belonging to a single operator [26], the transmission takes place in two phases. In the first phase, each terminal transmits to the relay using the same resources, so that their transmissions interfere. Assuming frequency-flat fading and denoting the channel between the k-th user of the ℓ-th operator and the relay by $\boldsymbol{H}_k^{(\ell)} \in \mathbb{C}^{M_\mathrm{R} \times M_k^{(\ell)}}$, where $k, \ell \in \{1, 2\}$, the signal received by the relay can be expressed as

$$\boldsymbol{r} = \boldsymbol{H}^{(1)} \cdot \boldsymbol{x}^{(1)} + \boldsymbol{H}^{(2)} \cdot \boldsymbol{x}^{(2)} + \boldsymbol{n}_\mathrm{R} \in \mathbb{C}^{M_\mathrm{R} \times 1}, \tag{6.5}$$

where $\boldsymbol{H}^{(\ell)} = \left[\boldsymbol{H}_1^{(\ell)}, \boldsymbol{H}_2^{(\ell)}\right]$ represents the concatenated MIMO channel of the ℓ-th operator, $\boldsymbol{x}^{(\ell)} = \left[\boldsymbol{x}_1^{(l)^\mathrm{T}}, \boldsymbol{x}_2^{(l)^\mathrm{T}}\right]^\mathrm{T}$ is the aggregate transmitted signal from each operator, and the vector $\boldsymbol{n}_\mathrm{R}$ is the noise component at the relay. Moreover, to simplify the notation, we assume that reciprocity is valid so that the backward channel between the relay and the k-th user of the ℓ-th operator is given by $\boldsymbol{H}_k^{(\ell)^\mathrm{T}}$. This assumption is fulfilled in a TDD system if identical RF chains are applied.

In the second transmission phase, the relay transmits to all terminals simultaneously. Since we assume an amplify and forward relay, the signal transmitted by the relay can be expressed as

$$\bar{\boldsymbol{r}} = \gamma \cdot \boldsymbol{G} \cdot \boldsymbol{r} \quad \text{for} \quad \boldsymbol{G} = \gamma_0 \cdot \boldsymbol{G}_\mathrm{T} \cdot \boldsymbol{G}_\mathrm{S} \cdot \boldsymbol{G}_\mathrm{R}. \tag{6.6}$$

Here, the parameter $\gamma_0 \in \mathbb{R}^+$ is chosen such that the relay amplification matrix $\boldsymbol{G} \in \mathbb{C}^{M_\mathrm{R} \times M_\mathrm{R}}$ is normalized to unit Frobenius norm. Moreover, $\gamma \in \mathbb{R}^+$ is the scaling factor used for adjusting the signal so that the transmit power constraint is fulfilled. The matrices $\boldsymbol{G}_\mathrm{T} \in \mathbb{C}^{M_\mathrm{R} \times 2M_\mathrm{R}}$ and $\boldsymbol{G}_\mathrm{R} \in \mathbb{C}^{2M_\mathrm{R} \times M_\mathrm{R}}$ represent the relay's receive

filter and transmit filter, respectively. Their task is to mitigate the inter-operator interference for each sub-system. The matrix $\boldsymbol{G}_{\mathrm{S}} \in \mathbb{C}^{2M_{\mathrm{R}} \times 2M_{\mathrm{R}}}$ is constructed via

$$\boldsymbol{G}_{\mathrm{S}} = \begin{bmatrix} \boldsymbol{G}_{\mathrm{S}}^{(1)} & \boldsymbol{0}_{M_{\mathrm{R}} \times M_{\mathrm{R}}} \\ \boldsymbol{0}_{M_{\mathrm{R}} \times M_{\mathrm{R}}} & \boldsymbol{G}_{\mathrm{S}}^{(2)} \end{bmatrix}, \tag{6.7}$$

where $\boldsymbol{G}_{\mathrm{S}}^{(1)}, \boldsymbol{G}_{\mathrm{S}}^{(2)} \in \mathbb{C}^{M_{\mathrm{R}} \times M_{\mathrm{R}}}$ are the relay amplification matrices for each sub-system. Note that $\boldsymbol{G}_{\mathrm{S}}$ is block diagonal since it represents the processing performed in the individual subsystems.

The transmit and receive filter matrices $\boldsymbol{G}_{\mathrm{T}}$ and $\boldsymbol{G}_{\mathrm{R}}$ can also be partitioned as

$$\boldsymbol{G}_{\mathrm{T}} = \begin{bmatrix} \boldsymbol{G}_{\mathrm{T}}^{(1)}, & \boldsymbol{G}_{\mathrm{T}}^{(2)} \end{bmatrix} \text{ and } \boldsymbol{G}_{\mathrm{R}} = \begin{bmatrix} \boldsymbol{G}_{\mathrm{R}}^{(1)^{\mathrm{T}}}, & \boldsymbol{G}_{\mathrm{R}}^{(2)^{\mathrm{T}}} \end{bmatrix}^{\mathrm{T}}, \tag{6.8}$$

where $\boldsymbol{G}_{\mathrm{T}}^{(\ell)} \in \mathbb{C}^{M_{\mathrm{R}} \times M_{\mathrm{R}}}$ and $\boldsymbol{G}_{\mathrm{R}}^{(\ell)} \in \mathbb{C}^{M_{\mathrm{R}} \times M_{\mathrm{R}}}$ for $\ell \in \{1, 2\}$.

After establishing the system model, in the next section, we focus on the question how to find the matrices $\boldsymbol{G}_{\mathrm{T}}$, $\boldsymbol{G}_{\mathrm{S}}$, and $\boldsymbol{G}_{\mathrm{R}}$.

6.4.2.2 Two-step algorithm

The separation of the the two sub-systems requires the suppression of the inter-operator interference. The scheme we propose here is inspired by the precoding technique BD that was first proposed in [28]. Via BD we force all the inter-operator interference to zero by choosing one operator's relay receive filter matrix $\boldsymbol{G}_{\mathrm{R}}^{(\ell_1)}$ such that it projects the signal into the null space of the other operator's channel matrices $\boldsymbol{H}^{(\ell_2)}$ for $\ell_1 \neq \ell_2$ and $\ell_1, \ell_2 \in \{1, 2\}$. Thereby, the received signal at the relay is decomposed into two parallel independent sub-systems. The projection matrix can for example be calculated from the SVD of $\boldsymbol{H}^{(\ell_2)}$, as in BD [28]. To ensure that the system seen by the users of each operator in the second transmission phase is also isolated from the inter-operator interference, the transmit filter matrix $\boldsymbol{G}_{\mathrm{T}}$ for the second ("downlink") phase needs to be applied. Due to the reciprocity of the channel, we can simply choose $\boldsymbol{G}_{\mathrm{T}} = \boldsymbol{G}_{\mathrm{R}}^{\mathrm{T}}$. However, we should be aware that the BD algorithm has a dimensionality constraint stating that the total accumulated number of antennas at each user terminal has to be less or equal than the number of antennas at the relay.

After canceling the interference between the operators, the overall received signal

in the downlink can be expressed as

$$\begin{aligned}\begin{bmatrix} \boldsymbol{y}^{(1)} \\ \boldsymbol{y}^{(2)} \end{bmatrix} &= \gamma \cdot \gamma_0 \cdot \begin{bmatrix} \boldsymbol{H}^{(1)^{\mathrm{T}}} \\ \boldsymbol{H}^{(2)^{\mathrm{T}}} \end{bmatrix} \cdot \boldsymbol{G}_{\mathrm{T}} \cdot \boldsymbol{G}_{\mathrm{S}} \cdot \boldsymbol{G}_{\mathrm{R}} \cdot \left[\boldsymbol{H}^{(1)} \boldsymbol{H}^{(2)}\right] \cdot \begin{bmatrix} \boldsymbol{x}^{(1)} \\ \boldsymbol{x}^{(2)} \end{bmatrix} + \begin{bmatrix} \tilde{\boldsymbol{n}}^{(1)} \\ \tilde{\boldsymbol{n}}^{(2)} \end{bmatrix} \\ &= \gamma \cdot \gamma_0 \cdot \begin{bmatrix} \boldsymbol{H}^{(1)^{\mathrm{T}}} \cdot \boldsymbol{G}_{\mathrm{R}}^{(1)^{\mathrm{T}}} \cdot \boldsymbol{G}_{\mathrm{S}}^{(1)} \cdot \boldsymbol{G}_{\mathrm{R}}^{(1)} \cdot \boldsymbol{H}^{(1)} & \mathbf{0} \\ \mathbf{0} & \boldsymbol{H}^{(2)^{\mathrm{T}}} \cdot \boldsymbol{G}_{\mathrm{R}}^{(2)^{\mathrm{T}}} \cdot \boldsymbol{G}_{\mathrm{S}}^{(2)} \cdot \boldsymbol{G}_{\mathrm{R}}^{(2)} \cdot \boldsymbol{H}^{(2)} \end{bmatrix} \\ &\quad \cdot \begin{bmatrix} \boldsymbol{x}^{(1)} \\ \boldsymbol{x}^{(2)} \end{bmatrix} + \begin{bmatrix} \tilde{\boldsymbol{n}}^{(1)} \\ \tilde{\boldsymbol{n}}^{(2)} \end{bmatrix}, \end{aligned} \tag{6.9}$$

where $\boldsymbol{y}^{(\ell)} \in \mathbb{C}^{(M_1^{(\ell)}+M_2^{(\ell)})\times 1}$ and $\tilde{\boldsymbol{n}}^{(\ell)} \in \mathbb{C}^{(M_{(\ell)}^{l}+M_2^{(\ell)})\times 1}$ are the signal and the effective noise term received by operator ℓ. Consequently, for each sub-system we obtain

$$\boldsymbol{y}^{(\ell)} = \gamma \cdot \gamma_0 \cdot \tilde{\boldsymbol{H}}^{(\ell)^{\mathrm{T}}} \cdot \boldsymbol{G}_{\mathrm{S}}^{(\ell)} \cdot \tilde{\boldsymbol{H}}^{(\ell)} \cdot \boldsymbol{x}^{(\ell)} + \tilde{\boldsymbol{n}}^{(\ell)}, \tag{6.10}$$

where the transformed channel matrices per operator are given by $\tilde{\boldsymbol{H}}^{(\ell)} = \boldsymbol{G}_{\mathrm{R}}^{(\ell)} \cdot \boldsymbol{H}^{(\ell)}$.

In order to find a suitable $\boldsymbol{G}_{\mathrm{S}}^{(\ell)}$ for each sub-system, any single-operator two-way relaying technique can be applied to the transformed channels $\tilde{\boldsymbol{H}}^{(\ell)}$, e.g., ZF or MMSE transceive filters [33]. However, in our simulations, we will use the ANOMAX strategy proposed in [26] due to its simplicity and its good performance compared to other single-operator two-way relaying transmit strategies.

6.4.3 Practical Implementation Issues

Unlike the relay scenario in Ch. 6.3, this scenario requires either perfect reciprocity of the MAC and BC channels or feedback of the channel coefficients, both from the UTs to the relay and from the relay to the UTs. Moreover, the relaying algorithm may require noise power estimates. In the following, the practical implementation issues are described in detail.

6.4.3.1 Imperfect Channel Reciprocity

Originally, the TWR algorithms are designed assuming perfect reciprocity of the MAc and the BC channels. However, the channel reciprocity is hard to fulfill, since the effective channel includes both the radio channel and the transfer functions of the RF chains. Generally, the transfer functions of the Tx- and Rx RF chains are different. Moreover, even if we assume the transfer functions of all RF chains to be identical[9], the received signals at the relay and those at the individual UTs contain different mixtures of the individual channels. The different mixtures result in different peak position of the mixed channel amplitude, causing difference of

[9]This has been demonstrated by FhG applying adequate RF calibration techniques.

signal frame starting point (identified via time synchronization) and thus, phase difference between MAC and BC channels as well as between the different channels associated to the different UTs in the BC phase. This effect destroys the reciprocity of the effective channels (obtained by channel estimation).

The most general and effective solution is to extend the relaying algorithms to the case without channel reciprocity. This is done by feeding back this problem to WP3. With this solution, the transmission will contain an extra BC-phase before the actual data transmission. First, a BC transmission of pilot signals is carried out to estimate the BC channels (and also the noise power at the UTs). Afterwards, the MAC phase pilot and data transmission is carried out, where the MAC channels (and the noise power at the relay) are estimated and the BC channel coefficients are fed back to the relay. Afterwards, the relay calculates the relay matrix based on the channel and noise power estimates. With this relay matrix, the relay transmits the signals in the BC phase. Both the data and the MAC channel estimates have to be sent. Finally, each UT decodes the signals using both the MAC and BC channel estimates.

In the case of assuming identical transfer functions of the RF chains, further simplification is possible to avoid the BC channel estimation. In this case, channel estimation has only to be carried out in the MAC phase. Afterwards, the possible mixtures of channels at the relay in the MAC phase as well as those at different UTs in the BC phase are calculated. With these mixtures, the relations of the peaks of these mixtures can be estimated. Correspondingly, the channel estimates are shifted accordingly for the relay matrix calculation, so that they can match the effective channels in the BC phase.

6.4.3.2 Time Synchronization Error

Except for the difference of channel mixtures mentioned in Sec. 6.4.3.1, time synchronization error can also cause difference of the signal frame starting point. We are planning to integrate additional Rx equalization to solve this problem. Further solutions are under investigation.

6.4.3.3 Colored Noise and Unequal Noise Power

The original designed relaying algorithm has assumed that the noise power at all UTs as well as at the relay is identical. However, this is not realistic. As mentioned before, the noise in practical systems is generally colored and consists narrow band interference. Moreover, the noise characteristic is generally different in different devices. Thus, the noise power values at different UTs and the relays are generally different. Moreover, the noise power values at different subcarriers are also different. Therefore, the relaying algorithm has to take this fact into account. After feeding this problem back to WP3, the relaying algorithms have been improved and can

cope with different noise power at different UTs and at the relay.

6.4.3.4 Rescaling of the Channel Coefficients or the Noise Power

In the relay, both the MAC and BC channel coefficients are used for the calculation the relaying matrix, which is used to precode the transmit signal of the relay in the BC phase. Similar to scenario SC2-TA and SC1-TB (see also 6.1.3.5), the BC channel for the calculation of the relay matrix has to be rescaled according to the amplitude scaling factor of the transmit signal in the BC phase. However, this scaling factor is unknown until the relay matrix is available. Thus, the same "deadlock" problem as in scenario SC2-TA and SC1-TB (see also 6.1.3.5) exists. Moreover, at each UT, the rescaled BC channel coefficients must be available, since they are further used to separate the desired signal stream from a mixture with the one sent by itself. The solutions in scenario SC2-TA and SC1-TB, i.e. using predefined scaling factor or iterative calculation, can be applied. The rescaling factor should be sent to the UTs, so that they can decode the received signal (in the BC phase). Since this information is the same for all UTs, the corresponding transmission is quite uncomplicated, i.e. with low overhead.

6.4.4 Mapping on the HIL-Demonstrator Platform

For the test of the SC1-TC-II scenario, the relay and the UTs are mapped to the demonstrator platform under the channel emulator mode. Due to the large number of Tx- and Rx antennas (8 Tx-/Rx antennas), different mappings are required in MAC and BC phases, as illustrated in Fig. 6.15. In this way, the physical transmitters and receivers can be reused. In the MAC phase, the 4 Tx antennas of the two experimental devices act the 4 single antenna UTs, while the 4 Rx antennas act the receiver of the relay (with 4 Rx antennas). In the BC phase, the roles of the Tx antennas and the Rx antennas are exchanged. The 4 Tx antennas and 4 Rx antennas of the platform are connected to the corresponding inputs and outputs of the channel emulator, respectively. To allow the remapping in the MAC and BC phases, normal channel emulation files can not be used, since they can emulate either the MAC or the BC channels. For the remapping, we need switching of the channels for the transition from MAC to BC or vice versa. This requires extension of the software generating the channel emulation files. This extension will be done in the future.

Fig. 6.38 shows the flowchart of the HIL test program. First, general parameter settings are carried out. Afterwards, the channel set up is carried out including the selection of the channel mode and the loading of the channel files. Afterwards, channel realization control and channel estimation are carried out. With each channel realization, different SNR levels are applied by adjusting the variable gain amplifiers at the modulators. For each channel realization and each SNR level, signal

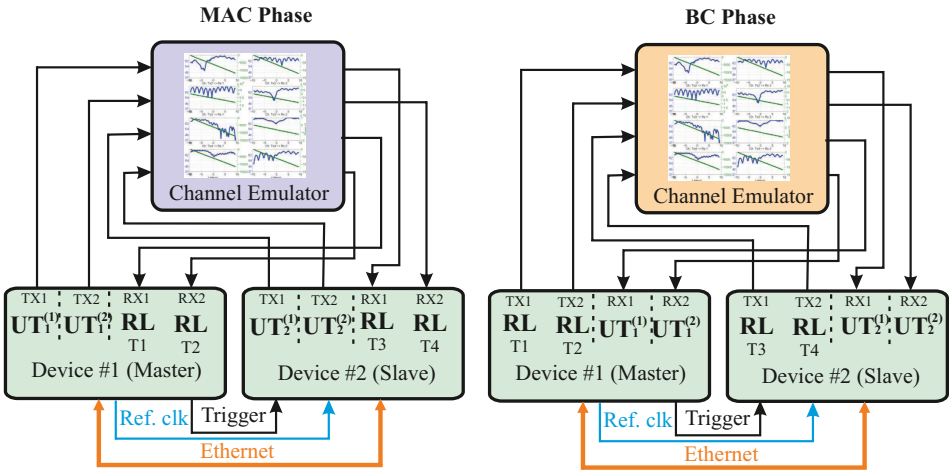

Figure 6.37: Mapping of scenario SC1-TC-II on the HIL platform with channel emulator mode

transmissions in the MAC and the BC phases with both non-spectrum sharing and spectrum sharing are carried out one after another. In the sharing case, different relay algorithms are applied. During each transmission, some intermediate results e.g. the received signal constellation and the currently measured throughput can be shown. After all transmissions are finished, the results will be evaluated and saved.

6.4.5 Initial HIL-Test Results

Since the implementation is still ongoing and the channel emulator function has to be modified, there are still no HIL test results available. However, after HIL experiments have been carried out, the HIL results will be shown in the final version of this deliverable i.e. D6.3b.

6.4.6 Future Works

First, the channel emulator extension has to be carried out, so that the remapping of the MAC- and the BC phases is allowed. Afterwards, systematic HIL test will be carried out to compare the non-spectrum-sharing case and the spectrum sharing case with different relaying algorithms incl. BD ANOMAX, RBD ANOMAX, excl. ANOMAX, ZF and MMSE. Finally, the HIL results will be evaluated.

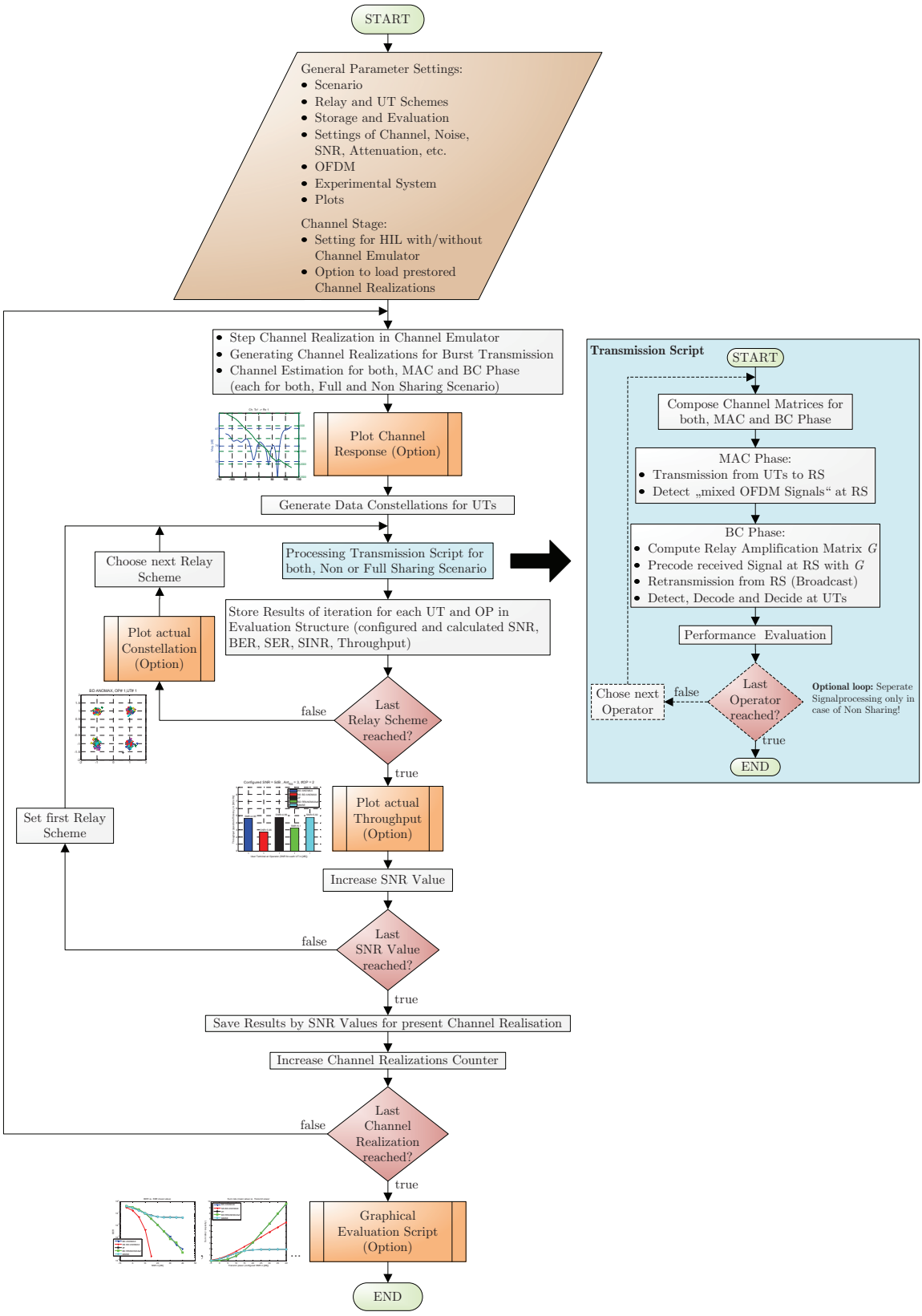

Figure 6.38: Flowchart of the software implementation of the TWR scenario.

7 Initial Implementation and Evaluation on the LTE-Advanced Testbed

7.1 Scenario SC2-TA: Spectrum Sharing

7.1.1 Scenario and Test Case Description

This scenario was already described in Sec. 6.1.1. However, we have chosen different test cases for the implementation on the LTE-Advanced testbed.

The initial test case for spectrum sharing in LTE-Advanced is the dynamical coordination of common spectrum access among mobile operators. This requires the dynamic exchange of information between the network operators, such as the instantaneous traffic served in each network and channel quality indicators (CQI) for terminals with high traffic demands. In this way, spectrum access can be dynamically coordinated among mobile operators. Despite common spectrum access, the shared spectrum is still used in an orthogonal way in this test case.

A further test case is to include non-orthogonal spectrum sharing. By introducing advanced multi-antenna techniques, spatial reuse of the radio resources is made possible. By exchange of channel state information (CSI) inside and between the networks, inter-cell interference cancellation is enabled. If user data are exchanged in addition, joint transmission coordinated multipoint (JT-CoMP) can be used. Fig. 7.1 illustrates this test case.

Since operators often use hardware from different vendors, the interfaces for the required information exchange need to be standardized and common rules for sharing the limited amount of radio resources have to be agreed on.

7.1.2 Mapping and Implementation on the LTE-Advanced Platform

The goal is to demonstrate that spectrum sharing can be realized in a distributed manner, in other words without any centralized control unit. This is an essential requirement for the feasibility of the approach in the distributed LTE network architecture. For simultaneous access to the compound spectrum by both operators, information is exchanged and common rules are defined. Two base stations exemplify two mobile operators. Operator 1 and Operator 2 do have 10 MHz bandwidths each at center frequencies 2.55, and 2.65 GHz. Eight frequency sub-bands can be assigned within each part of the spectrum. Terminals measure the current traffic

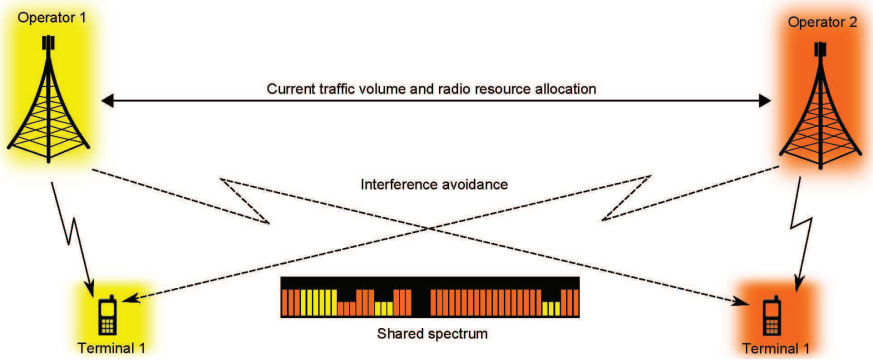

Figure 7.1: Spectrum sharing scenario on the LTE-Advanced testbed.

volume and the feasible data rate and feed it back over the up-link together with the current resource map. Measuring this information at the terminals was easier from an implementation point of view as normally this information is already given at the serving base station.

Operators exchange this information over the network interconnect. Each base station calculates the capacity consumed in each network from both resource maps and knows which resources can be assigned additionally in their own and in the other operator parts of the spectrum.

In a following stage, the resources are assigned individually by each network following a common set of rules. This is done by switching data streams on or off using a linear pre-coder at the transmitter side.

The following common rules have been implemented in the live demonstration:

1. Each operator starts by using its own resources first, as long as traffic is smaller than the capacity limit;
2. Unused resources in the compound spectrum are assigned by a fixed rule only if an operator's own resources are completely consumed;
3. If additional resources are no longer used, the worst resource is always released, i.e. sharing is opportunistic and channel-aware;
4. Resources are given back to the spectrum owners if they require additional spectrum room, but there are no more free resources available in the compound spectrum;
5. If the load is simultaneously high in both networks, operators move back to their own parts of the spectrum. The last two rules are needless in LTE Rel. 11/12 if CSI is available at base stations and inter-cell interference cancellation techniques can be used.

Fig. 7.2 shows a screenshot of the live demonstration. As we can see, the allocated frequency resources for the two operators are shown on the left- and the right hand

side of this figure. The allocated amount of frequency resources scales with the data load, which can be seen from the number of active UTs as well as the video streams of each operator (lower part of the figure). By using the frequency resource of operator 2, the data throughput of operator 1 can be enhanced to cope with the high load.

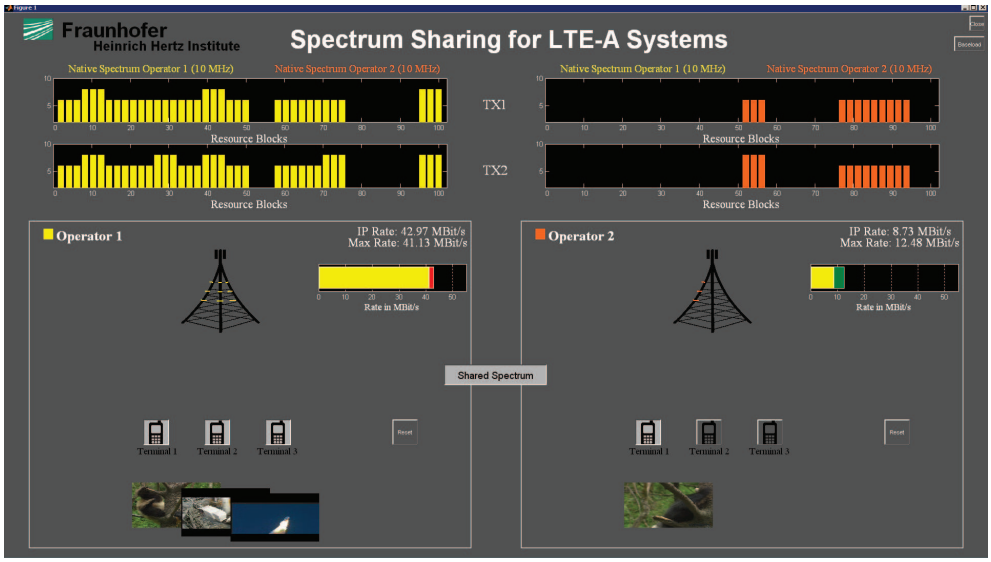

Figure 7.2: Screenshot of the initial LTE-Advanced demonstration on spectrum sharing.

8 Summary and Conclusions

In this deliverable, the results and progress of the initial scenario and test case implementation and evaluation on the demonstrator testbed are reported. First, an overview of the selected scenarios and test cases for implementation is given. Afterwards, the scenario implementation work flow is described, which includes the interaction between WP6 and the other WPs. The important functionalities of the HIL-demonstrator platform as well as the LTE-Advanced testbed are described. For HIL-demonstrator platform, the test case implementation and evaluation of four scenarios are reported. The first one is the spectrum sharing scenario without base-station collocation. The second one is the full sharing (spectrum and base-station) scenario. In both these scenarios, advanced beam-forming techniques were applied to enable SAPHYRE gains with sharing. HIL test results show that by sharing the spectrum, considerable gain in rate/throughput can be achieved. Moreover, especially in the first scenario, a number of advanced beam-forming algorithms have been applied. By comparing their performance, we found out the the better the performance, the higher the required computational complexity. Thus, a tradeoff between performance and complexity has to be made by selecting the techniques. The third and the fourth scenarios are both relay sharing scenarios, while the third scenario consists of a "butterfly" network, the fourth scenario consists a two-way-relaying network. In the third case, advanced network coding techniques were applied to enable spectrum sharing. In the fourth case, advanced multi-antenna techniques were applied at the relay to allow spectrum sharing gain. HIL test results has verified the sharing gain in the third scenario. For the fourth, the HIL test remains future work. Moreover, the implemented scenarios and test cases will be further improved and refined. More algorithms are expected to be included in the different scenarios. The corresponding HIL tests and evaluation will be carried out. Furthermore, a subset of the selected scenarios will be implemented and evaluated on a LTE-Advanced testbed. The corresponding experimental setup, test case definition and the initial implementation were described.

Bibliography

[1] Fahldieck, Torsten and Haibin Zhang et al.: *Resource allocation and interference management strategies*, 2011.

[2] Fettweis, Gerhard, Michael Löhning, Denis Petrovič, Markus Windisch, Peter Zillmann, and Wolfgang Rave: *Dirty RF: a new paradigm.* In *Proc. of IEEE International Symposium on Personal, Indoor and Mobile Radio Communications (PIMRC)*, volume 4, pages 2347–2355, September 2005.

[3] Gesbert, David, Jacek Kibilda, and Martin Haardt et al.: *Saphyre reference scenario parameters and novel interference models (initial)*, 2010.

[4] Haardt, Martin, Zuleita Ka Ming Ho, Eduard Jorswieck, and et al.: *Saphyre project deliverable d3.1a: Adaptive and robust signal processing in multi-user and multi-cellular environments (initial)*, 2010.

[5] Ho, Zuleita K. M., Mariam Kaynia, and David Gesbert: *Distributed power control and beamforming on MIMO interference channels.* In *Proc. of IEEE European Wireless Conference (EW)*, pages 654–660, April 2010.

[6] Janssen, Thom, Adrian Pais, and Haibin Zhang et al.: *Initial reference scenarios for resource sharing*, 2010.

[7] Jehle, Geoffrey A. and Philip J. Reny: *Advanced Microeconomic Theory.* Addison-Wesley. Pearson Education, 2nd edition, 2003.

[8] Jorswieck, E. A., E. G. Larsson, and D. Danev: *Complete characterization of the Pareto boundary for the MISO interference channel.* IEEE Trans. Signal Process., 56(10), Oct. 2008, ISSN 1053-587X.

[9] Jorswieck, Eduard A.: *Framework for beamforming in interference networks: Multicast, MISO IFC and secrecy capacity.* In *International Zürich Seminar on Communications*, 2010.

[10] Jorswieck, Eduard A., Leonardo Badia, Torsten Fahldieck, David Gesbert, Stefan Gustafsson, Martin Haardt, Ka Ming Ho, Eleftherios Karipidis, Andreas Kortke, Erik G. Larsson, Hrjehor Mark, Maciej Nawrocki, Radoslaw Piesiewicz, Florian R¨omer, Martin Schubert, Jan Sykora, Peter Trommelen, Bram van den Ende, and Michele Zorzi: *Resource sharing in wireless networks: The SAPHYRE approach.* In *Proc. of Future Network and Mobile Summit (FNMS)*, pages 1–8, June 2010.

[11] Jungnickel, V. and et al.: *Field trials using coordinated multi-point transmission in the downlink.* In *PIMRC'10 Workshops*, sept. 2010.

[12] Kyosti, Pekka, Juha Meinila, and Lassi Hentila et al.: *Winner ii project deliverable d1.1.2: WINNER II channel models.* /www.ist-winner.org, 2007.

[13] Larsson, E. G. and E. A. Jorswieck: *Competition versus cooperation on the MISO interference channel.* IEEE Journal on Selected Areas in Comm., September 2008.

[14] Li, Jianhui, Florian Römer, and Martin Haardt: *Linear precoding design in MIMO interference relay channels.* In *Proc. of IEEE International Conference on Acoustics, Speech and Signal Processing (ICASSP)*, May 2011.

[15] Lindblom, J. and E. Karipidis: *Cooperative beamforming for the MISO interference channel.* In *European Wireless'10*, Lucca, Italy, 2010.

[16] Luo, Jian and Andreas Kortke: *Saphyre project deliverable d6.2: Internal report on demonstrator platform development*, 2010.

[17] Luo, Jian, Andreas Kortke, and Wilhelm Keusgen: *Efficient channel estimation schemes for MIMO OFDM systems with NULL subcarriers.* In *Proc. of IEEE Vehicular Technology Conference (VTC)*, pages 1–5, September 2008.

[18] Luo, Jian, Andreas Kortke, Wilhelm Keusgen, Jianhui Li, Martin Haard, Rami Mochaourab, Eduard Jorswieck, Johannes Lindblom, Eleftherios Karipidis, and Erik G. Larsson: *Advanced beam-forming techniques for inter-operator spectrum sharing: From theory to practice.* Future Network and Mobile Summit Conference Proceedings, Berlin, Germany, 2012. submitted.

[19] Luo, Jian, Andreas Kortke, Wilhelm Keusgen, Jianhui Li, Martin Haardt, Pavel Prochazka, and Jan Sykora: *A flexible hardware-in-the-loop test platform for physical resource sharing mechanisms in wireless networks.* In *Proc. of Future Network and Mobile Summit (FNMS)*, June 2011.

[20] Luo, Jian, Andreas Kortke, Jianhui Li, Pavel Prochazka, and Jan Sykora: *Saphyre project deliverable d6.1a: Scenario definition and test case selection for demonstrator platform evaluation*, 2010.

[21] Mochaourab, R. and E. A. Jorswieck: *Exchange economy in two-user multiple-input single-output interference channels.* IEEE J. Sel. Topics Signal Process., 2011, ISSN 1932-4553. accepted for publication.

[22] Mochaourab, R. and E. A. Jorswieck: *Optimal beamforming in interference networks with perfect local channel information.* IEEE Transactions on Signal Processing, March 2011.

[23] Mochaourab, Rami and E. A. Jorswieck: *Walrasian equilibrium in two-user multiple-input single-output interference channel.* In *Proc. ICC*, Kyoto, Japan, 2011.

[24] Mochaourab, Rami, E. A. Jorswieck, Ka Ming Zuleita Ho, and D. Gesbert: *Bargaining and beamforming in interference channels.* In *Proc. Asilomar*, Nov. 2010.

[25] Popovski, Petar and Hiroyuki Yomo: *Physical network coding in two-way wireless relay channels.* In *Proc. of IEEE International Conference on Communications (ICC)*, pages 707–712, June 2007.

[26] Roemer, F., E. Jorswieck, and M. Haardt: *Efficient spatial processing and resource allocation for amplify and forward two-way relaying.* Cross Layer Designs in WLAN Systems, N. Zorba and C. Skianis and C. Verikoukis, eds., Troubador Publishing Ltd, Leicester, UK, Sep. 2010.

[27] Römer, Florian, Jianshu Zhang, Martin Haardt, and Eduard Jorswieck: *Spectrum and infrastructure sharing in wireless networks: A case study with relay-assisted communications.* In *Proc. of Future Network and Mobile Summit (FNMS)*, June 2010.

[28] Spencer, Q. H., A. L. Swindleherst, and M. Haardt: *Zero-forcing methods for downlink spatial multiplexing in multiuser MIMO channels.* IEEE Trans. Signal Process., Feb. 2004.

[29] Stankovic, V. and M. Haardt: *Generalized design of multi-user MIMO precoding matrices.* IEEE Trans. on Wireless Commun., 7, March 2008.

[30] Stege, Matthias, Frank Schafer, Matthias Henker, and Gerhard Fettweis: *Hardware in a loop-a system prototyping platform for MIMO-approaches.* pages 216–222, March 2004.

[31] Sykora, Jan and Alister Burr: *Network coded modulation with partial side-information and hierarchical decode and forward relay sharing in multi-source wireless network.* In *Proc. of IEEE European Wireless Conference (EW)*, pages 1–7, April 2010.

[32] Sykora, Jan, Miroslav Hekrdla, Pavel Prochazka, and Tomas Uricar: *Network, resource, and interference aware coding and decoding (initial)*, 2010.

[33] Unger, T. and A. Klein: *Duplex schemes in multiple antenna two-hop relaying.* EURASIP Journal on Advances in Signal Processing, 2008.

[34] Zu, Lijun, Ping Wang, Jing Han, Fuqiang Liu, Qing Ai, and Yusheng Ji: *A study on test platform for verifying new wireless networking technologies via hardware-in-loop simulation.* In *Proc. of International Conference on Cyber-Enabled Distributed Computing and Knowledge Discovery (CyberC)*, pages 75–78, October 2010.